

# Neutrino Detectors and Sources

April 20, 2016

## Contents

<b>1</b>	<b>Introduction</b>	<b>3</b>
<b>2</b>	<b>Methods of Neutrino Detection</b>	<b>3</b>
2.1	The Radiochemical Technique . . . . .	3
2.1.1	The Homestake Experiment . . . . .	4
2.1.2	SAGE, Gallex and GNO . . . . .	4
2.1.3	What you need to know . . . . .	4
2.2	Water Cerenkov Technique . . . . .	4
2.2.1	SuperKamiokande . . . . .	7
2.2.2	Sudbury Neutrino Observatory, SNO . . . . .	7
2.2.3	What you need to know . . . . .	8
2.3	Scintillation Technique . . . . .	8
2.3.1	KamLAND . . . . .	9
2.3.2	What you need to know . . . . .	9
2.4	Tracking and Hybrid Detectors . . . . .	9
2.4.1	What you need to know . . . . .	12
<b>3</b>	<b>Natural Neutrino Sources</b>	<b>12</b>
3.1	Relic Neutrinos . . . . .	12
3.1.1	What you need to know . . . . .	13
3.2	Solar Neutrinos . . . . .	13
3.2.1	The Solar Neutrino Detectors and the Solar Neutrino Problem . . . . .	15
3.2.2	What you need to know . . . . .	16
3.3	Neutrinos From Supernovae . . . . .	17
3.3.1	The evolution of massive stars . . . . .	18
3.3.2	Core Collapse . . . . .	19
3.3.3	Supernova SN1987A . . . . .	20
3.3.4	What you need to know . . . . .	21
3.4	Other Astrophysical Neutrinos Sources . . . . .	21
3.4.1	Neutrinos produced in acceleration processes . . . . .	22
3.4.2	ANTARES, NESTOR and Baikal . . . . .	23
3.4.3	ICECUBE . . . . .	24
3.4.4	What you need to know . . . . .	24
3.5	Geoneutrinos . . . . .	24

3.5.1	What you need to know . . . . .	25
3.6	Atmospheric Neutrinos . . . . .	25
3.6.1	Atmospheric Neutrino Detectors and the Atmospheric Neutrino Anomaly . . . . .	27
3.6.2	What you need to know . . . . .	29
<b>4</b>	<b>Artificial Neutrino Sources</b>	<b>29</b>
4.1	Reactors . . . . .	29
4.1.1	What you need to know . . . . .	31
4.2	Neutrino Beamlines . . . . .	31
4.2.1	Target . . . . .	31
4.2.2	Decay pipe . . . . .	32
4.2.3	Energy Spectrum . . . . .	32
4.2.4	Wide Band Beams . . . . .	33
4.2.5	Narrow Band Beams . . . . .	34
4.3	Off-axis beams . . . . .	36
4.3.1	What you need to know . . . . .	38
<b>5</b>	<b>What you should know (Summary)</b>	<b>38</b>

# 1 Introduction

Neutrinos are everywhere. They are generated in the sun, in extensive cosmic ray airshowers, in supernovae. We make them in nuclear reactors and in particle accelerators. There are even neutrinos still left over from the Big Bang around us. This section looks at some of the source of neutrinos and methods we use to detect them.

## 2 Methods of Neutrino Detection

We observe particles in our detectors by the way that they interact with matter. For example, an electron is observed because it bends in magnetic fields and can ionise gas in drift chambers due to the fact that it is electrically charged. This is all depends on the particle having some property which can interact with the matter around it : for most particles this is either electrical charge or mass. The neutrino is neutral and has a very small mass and is therefore for all intents and purposes invisible. We must infer the presence of a neutrino by the particles it leaves behind after it has undergone an interaction. As an example, if a  $\nu_\mu$  scatters quasielastically off a neutron ( $\nu_\mu + n \rightarrow \mu^- + p$ ), we are left with a visible charged muon and proton. If we can reconstruct these tracks, we can infer the presence of a  $\nu_\mu$  and even recognise that the interaction was a quasielastic scatter by analysis of the kinematics of the final state. This would tend to suggest that the sort of detectors we want to build are low mass detectors with extremely fine tracking capability. Unfortunately the other constraint we have is the size of the neutrino cross section. Since this is so small we need to build large, high mass detectors to be have a large enough event rate to perform useful studies. The sort of neutrino detectors we actually build seek to combine high mass targetry with fine grained particle tracking and identification - not always successfully. There are essentially four different methods used to detect neutrinos. Which method you choose depends on a number of things including, but not limited to

- How many events do you want and with what energy of neutrino? This determines the mass of your detector.
- What kind of interaction do you want to look at ?  $\nu_e, \nu_\mu, \nu_\tau$ ? Charged current or Neutral current?
- What final state do you want to detect and what do you want to measure in this final state? This will affect detector technology choices.
- What sort of background do you expect and how well do you need to eliminate them? This also influence detector technology, frequently conflicting with the choice you would have made in the last point.
- How much cash do you have? How much time?

### 2.1 The Radiochemical Technique

The radiochemical technique was the first method used to study low energy solar neutrinos. The principle is the inverse beta decay reaction



where the daughter nucleus  ${}^A_{N-1}(Z+1)$  is unstable and decays with a reasonably short half-life. These experiments usually detect that an electron neutrino has interacted by looking for the radioactive decay of the daughter nucleus. The technique is one of extremely low rates; for example, given an incident neutrino flux of about  $10^{10}\text{cm}^{-2}\text{s}^{-1}$ , and a cross-section on the order of  $10^{-45}\text{cm}^2$ , about  $10^{30}$  atoms are needed to produce a rate of one event per day. Such low event rates require a new unit, called the SNU :  $1\text{ SNU} = 10^{-36}$  interactions per target atom per second. These experiments tend to be large and cheap. They work by letting the number of daughter nuclides accumulate over a time that is small compared to the daughter decay time. Periodically the entire detector is flushed and the number of daughter nuclides counted, usually using complicated chemical processes. The only information this technique can give you is the number of electron neutrino interactions in a given time; all other information, neutrino energy, interaction time, neutrino direction and data concerning muon and tau neutrinos is lost.

### 2.1.1 The Homestake Experiment

The first and longest running solar neutrino experiment is the Homestake experiment built by Ray Davis in 1968. The reaction it used to detect the neutrinos was



which has an energy threshold of 814 keV. The detection method utilises the decay



which results in 2.82 keV X-ray emission. Operating in the Homestake goldmine in South Dakota, it consists of a 615 tonne tanks of cleaning fluid (perchlorate-ethylene). The argon atoms were extracted every 60 days or so. The detector is capable of measuring the decay of a single argon atom every two days. The results from the Homestake experiment will be discussed below in the context of the Solar Neutrino problem.

### 2.1.2 SAGE, Gallex and GNO

Three other experiments used the same sort of technique, but with different nuclei. The Gallium experiments used the reaction



which has a much lower threshold of 233 keV. With this threshold the gallium experiments were able to probe the so-called pp solar neutrino flux (see below).

### 2.1.3 What you need to know

- How this technique works, and what are its drawbacks.
- Which experiments use the technique.

## 2.2 Water Cerenkov Technique

When a charged particle travels through a medium faster than the speed of light in that medium, it radiates a cone of Cerenkov light. This cone is aligned to the direction of motion of the particle and

has an opening angle that is a function of the velocity of the particle and the refractive index of the medium

$$\cos\theta_c = \frac{1}{n\beta} \text{ where } \beta = \frac{v}{c} \tag{5}$$

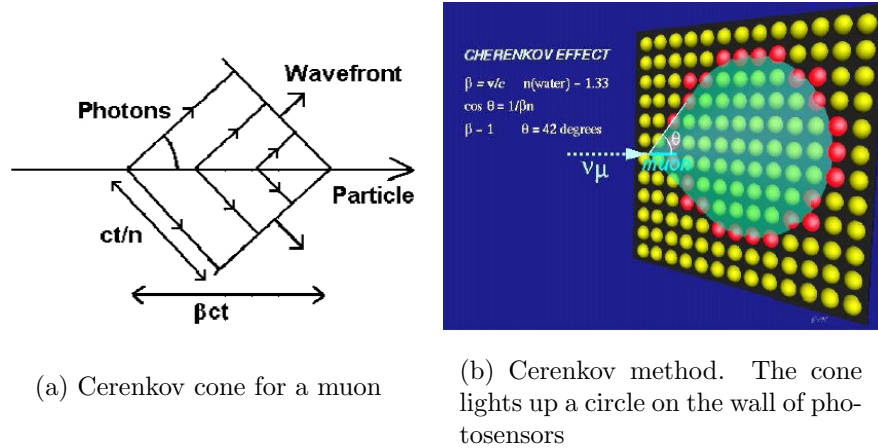


Figure 1: Detection principle of water Cerenkov detectors.

If one surrounds the target with light sensors, the cone will be detected as a circle of light as shown in Figure1. From the pattern of hits one can reconstruct the direction and energy of the particle that formed the ring. Particle identification is much harder and in most cases (for example, distinguishing a muon from a pion) is all but impossible. However, it is possible to distinguish electromagnetic particles from muon-like particles by the shape of the ring outline as shown in Figure2.

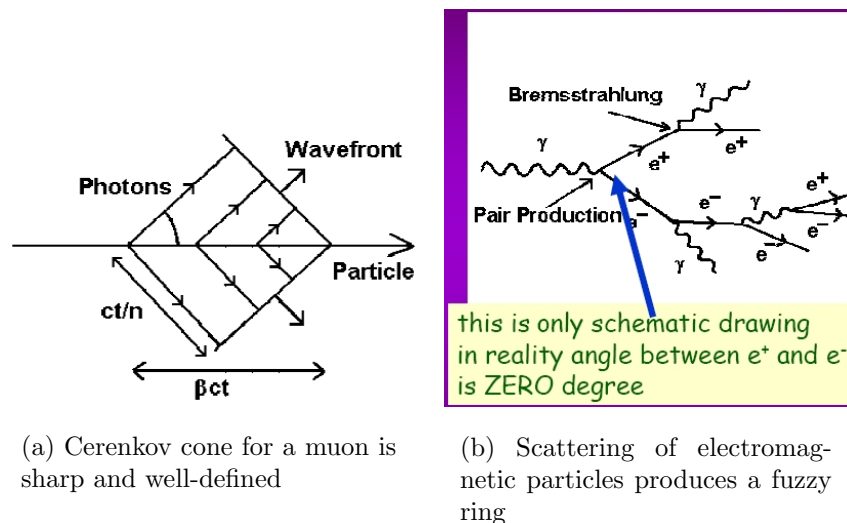


Figure 2: Distinguishing a photon from a muon in a water Cerenkov detector.

Electromagnetic particles tend to scatter in the target medium, leading to fuzzy rings, rather than the sharp edged rings seen with muon-like particles. The two plots in Figure3 show the hit pattern

seen in the Super-Kamiokande detector (which we'll talk about in a minute) for an electron-like (top) and muon-like (bottom) particle. Since the whole detection method relies on light travelling through the target medium, the medium must be highly transparent. There must also be a lot of it, to provide enough target mass, so it must be relatively cheap too. The best target material for these types of detectors is generally water. The disadvantage with this type of detector is that it cannot detect neutral particles, or charged particles below the Cerenkov threshold. Further, one generally has to reconstruct the ring pattern. This is easy for one ring events, and even two ring events, but as the number of particles increase the number of rings increases as well and the reconstruction complexity makes the task much more difficult. In general only low-multiplicity interactions with 2 or 3 particles can be reliably reconstructed.

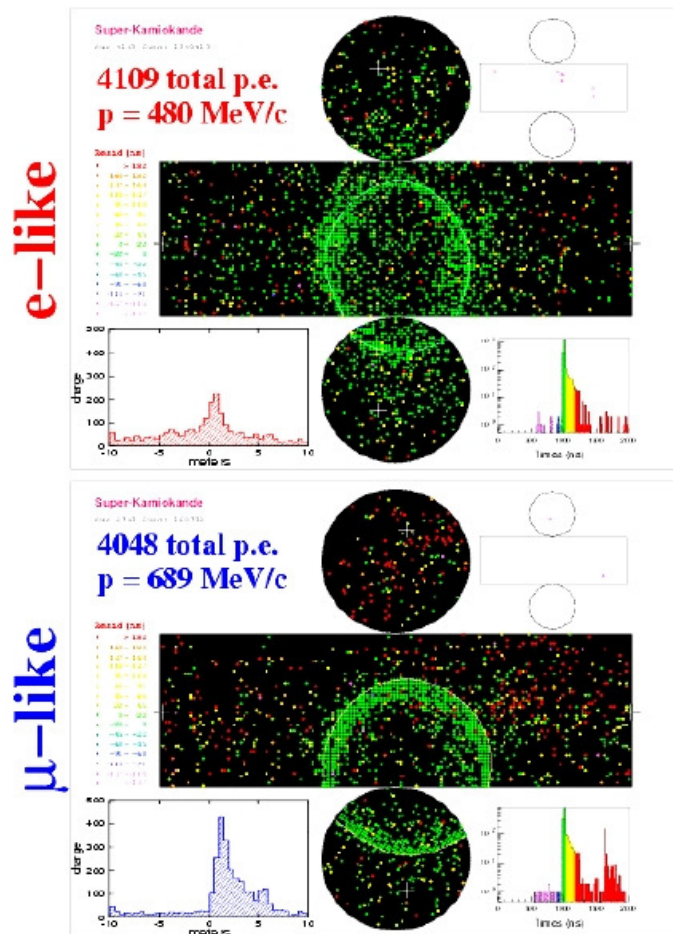


Figure 3: On the top - the hit pattern in the Super-Kamiokande detector from an electron-like particle showing the fuzzy ring signature. On the bottom, for comparison, is the hit pattern from a muon stopping in the detector.

The top plot shows the fuzzy ring of an electron (e-like) event and the bottom the sharply defined ring of a muon-like event which stops in the detector. The particle clearly stopped as the center of the ring sees no light, implying that at some point the particle went below threshold and stopped radiating. We will now discuss two of the most influential detectors of this type in particle physics today.

### 2.2.1 SuperKamiokande

From the point of view of neutrino physics, Super-Kamiokande is probably the most important experiment in the last 20 years. Designed to look for proton decay, the data it provided gave the best indications that the Solar Neutrino problem, and the Atmospheric Neutrino problem (see below) were both caused by neutrino flavour oscillations. It has been in operation since 1985.

The detector (see Figure 4) is a 50 kton cylindrical volume of ultra-pure water. It is 41.4 m high and 39.3 m in diameter and is viewed by 11,147 50-inch diameter photomultiplier tubes, which are mounted on the inner surfaces of the cylinder. Each photomultiplier is designed to be able to detect a single photon of light.

Super-Kamiokande is placed in the Kamioka mine, about 1 km underground, to provide a lot of shielding against particles produced in cosmic ray interactions in the atmosphere. Only neutrinos from cosmic ray showers, and very high energy muons, can reach the detector.

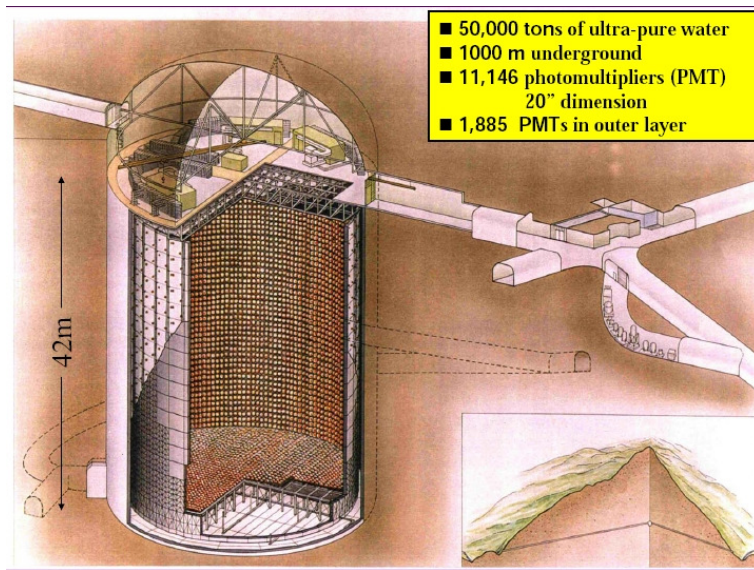


Figure 4: An artist's impression of the Super-Kamiokande detector.

The detector was designed to search for events in which there are only a few particles. It is usually used to tag the leading lepton in any interaction in the water, as that is almost always above threshold. This implies that Super-Kamiokande has very good efficiency for charged current interactions but is blind to neutral current interactions. Nevertheless, it is a staggeringly beautiful detector, as you can see from a photograph taken whilst the tank was being filled in Figure 5.

### 2.2.2 Sudbury Neutrino Observatory, SNO

About 2 kilometers underground, SNO is a large Cerenkov detector placed deep in a salt mine in Sudbury, Canada. It differs from Super-Kamiokande in that the target is 1000 t of heavy water, D<sub>2</sub>O, rather than normal plain water, H<sub>2</sub>O. This target is viewed by 9700 photomultipliers and is surrounded by a further 3 kilotonnes of normal water for shielding. The heavy water target gives SNO one advantage over Super-Kamiokande - it can observe neutral current interactions as well as charged current interactions. SNO is sensitive to charged current interactions involving on electron neutrinos via the absorption reaction  $\nu_e + d \rightarrow e + p + p$  which has a threshold of 1.4 MeV. In addition,

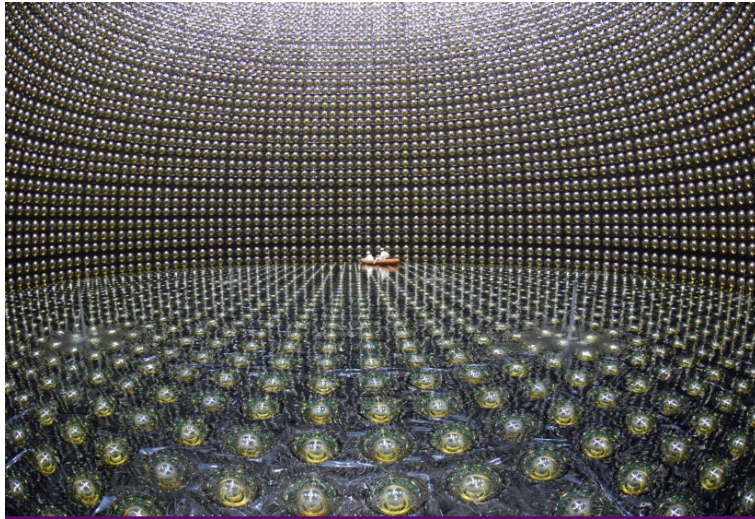


Figure 5: A photograph of the interior of Super-Kamiokande during water filling. The people on the boat are cleaning photosensor surfaces as the water level slowly rises. It takes about a week to fill the tank.

it is sensitive to all the neutrino flavours through the elastic scattering channel,  $\nu + e^- \rightarrow \nu + e^-$ . The unique aspect of SNO comes from its sensitivity to neutral current interactions via the reaction  $\nu + d \rightarrow \nu + p + n$ . The neutron produced in this interaction is detected via the 6.3 MeV gamma rays produced in the auxiliary reaction  $n + d \rightarrow H^3 + \gamma$ . This capability is extremely important for the study of solar neutrinos, as we will see later.

### 2.2.3 What you need to know

- How this technique works, and what are its benefits and drawbacks.
- How do you do particle identification with this technique? Can you identify everything or just muon- and electron-like particles.
- Which experiments use the technique.
- What distinguishes SNO from SuperK?

## 2.3 Scintillation Technique

The process of scintillation is a chemical process of luminescence whereby light of a characteristic spectrum is emitted following the absorption of radiation. This radiation is usually of a higher energy than the emission. Scintillation light is isotropic and generally has a very small (or no) energy threshold. This latter quality means that a detector using scintillator as the active material would be able to detect particles down to very low energies, distinguishing them from water Cerenkov detectors with their relatively high Cerenkov threshold. Scintillators are available in a range of materials : inorganic crystals (NaI is a common one), organic plastics, which are robust and easy to manipulate, but tend to lose light yield as they age, and organic liquids, where the scintillating material is dissolved in a bulk carrier such as mineral oil. Liquid scintillators can be quite toxic.



Scintillator detectors generally use the same principle as water Cerenkov detectors. The scintillator is enclosed in a large volume. The inner walls of the volume are covered with photosensors to observe the scintillation light. The isotropy of scintillation light means that scintillator detectors cannot reconstruct particle direction as well as water Cerenkov. If the volume enclosing the scintillator is reasonably small, however, relative timing of each hit can be used to estimate the position at which the particle started moving the scintillator.

Scintillator detectors are usually used to view electron antineutrinos being emitted from reactors. As discussed below, neutrinos from reactors tend to have energies around 2-3 MeV. This is too low for water Cerenkov detectors, but visible to the scintillator detectors.

### 2.3.1 KamLAND

The scintillator detector, KamLAND, rests in the Kamioka mine in Japan, a few hundred meters from the location of Super-Kamiokande. The detector was designed to observe electron antineutrinos being emitted from nuclear reactors around Japan, a free source of neutrinos. The goal of the experiment was to conclusively study the flavour oscillation of neutrinos with the same sort of parameters as those which come from the sun (more on this later).

The detector itself consists of 1000 tonnes of liquid scintillator contained within a spherical weather balloon. This balloon is surrounded by a non-scintillating fluid for shielding and is viewed by 1280 phototubes. The balloon is just thin enough to allow scintillating light to be visible to the photosensors through the balloon material, whilst thick enough to be able to support the scintillator liquid - a difficult balancing act (see Figure 6).

The electron antineutrino signal is obtained from the coincidence of two reactions : the first being the annihilation of the positron from the inverse beta decay reaction  $\bar{\nu} + p \rightarrow n + e^+$ . The neutron from this reaction is then captured by a free proton about 10-100  $\mu s$  later, yielding a 2.2 MeV photon :  $p + n \rightarrow d + \gamma$ . The time coincidence and energy measurement of the final state photon is the main indication that an electron antineutrino has interacted in the scintillator.

The detector is able to see electron antineutrinos from nuclear reactors up to 150 km from the Kamioka mine, and is also able to probe the solar neutrino flux to a lower energy threshold than Super-Kamiokande or SNO using the reaction  $\nu_e + e^- \rightarrow \nu_e + e^-$ , albeit with far less signal purity and more background issues from materials in the detector which can also radioactively decay. This signal will not produce the neutron that the inverse beta decay reaction relies on, and is just a single flash of light in the detector, with many background sources that mimic it. There is no trick to bringing this background down apart from ensuring that everything in your detector is made out of materials which are stable and contain no radioactive components (a difficult task as everything has traces of radioactive elements).

### 2.3.2 What you need to know

- How this technique works, and what are its benefits and drawbacks.

## 2.4 Tracking and Hybrid Detectors

The final technique we will investigate is used in high energy applications, where the neutrino energy is above a few GeV. In this case what one generally wants to do is to track each particle that is produced in the interaction. The general design is shown in Figure 7. In such a detector, there can be passive layers separated by active layers which perform the actual detection. The passive layers are

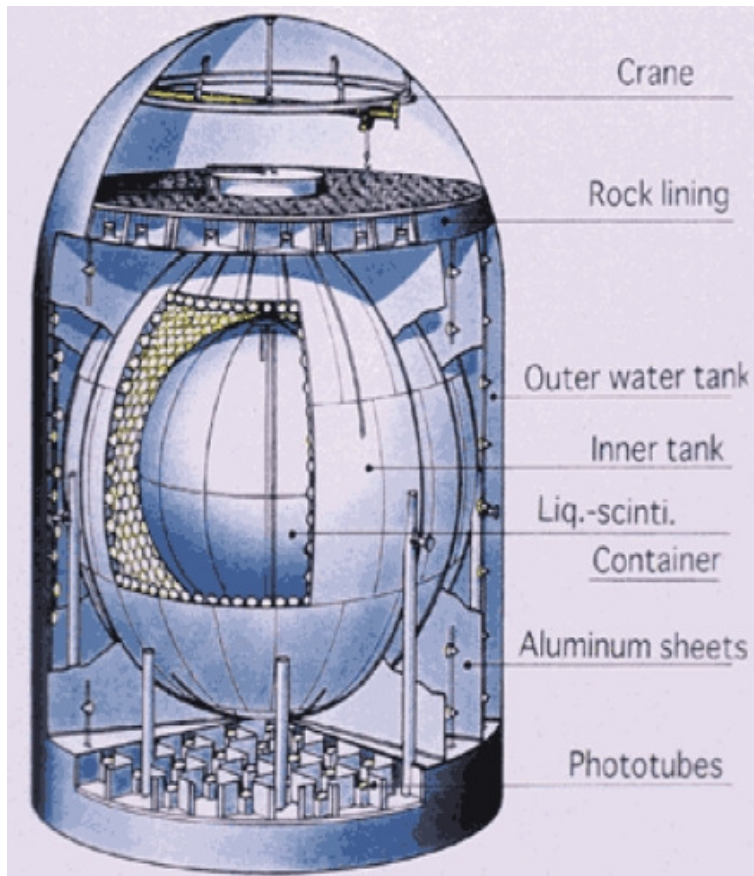


Figure 6: A diagram of the KamLAND detector showing the inner balloon containing the liquid scintillator surrounded by the photosensor sphere.

there to stop particles quickly in order to obtain an estimate of their momentum. Technologies for the active layers are myriad - drift tubes, spark chambers, scintillating bars, resistive plate chambers - basically any technology that will generate a signal when a charged particle goes through it and which can give reasonable position resolution.

Particle energy is measured through three main routes, depending on particle type : range, magnetic tracking and shower calorimetry. Going through each of these takes us too far off the discussion (and would involve about another 80 pages to do justice - shower calorimetry, for example, is the subject of entire books).

An example of this type of detector is NuTeV. NuTeV was a long detector composed of iron plates as the target interspersed with scintillator and drift chambers for tracking. A diagram of NuTeV is shown in Figure 8. Designed to look at high energy, Deep Inelastic Scattering events, the first part of the detector provides target mass for the neutrino beam and the second part forms a magnetic channel, which bends muons as they enter and provides momentum measurement. The hadronic part of the interaction interacts, and is contained, in the iron. A sample event display is shown in Figure 9 showing the long muon bending as it goes through the magnetic channel, and the short hadronic shower splash near the vertex.

Finally, there is a class of detectors which mimic the sort of design seen collider detectors. These have fine-grained tracking, muon spectrometers, hadronic and electromagnetic calorimetry and par-

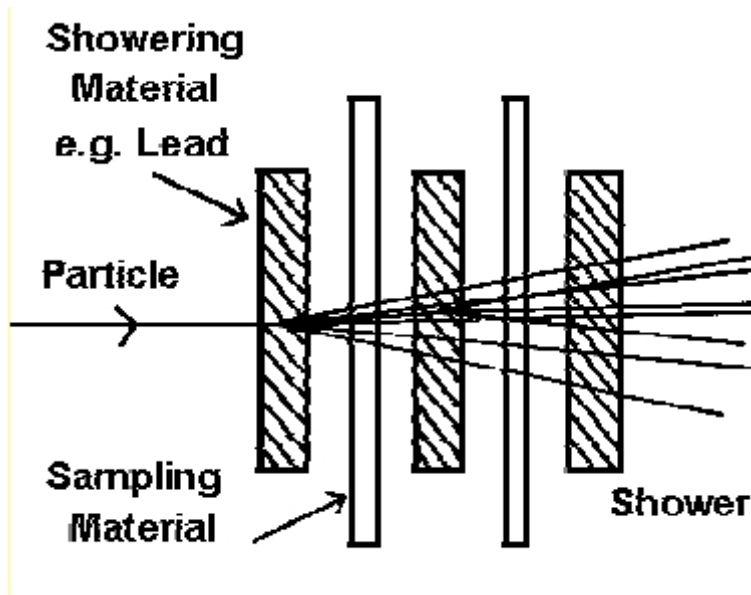


Figure 7: General design of a sampling detector.

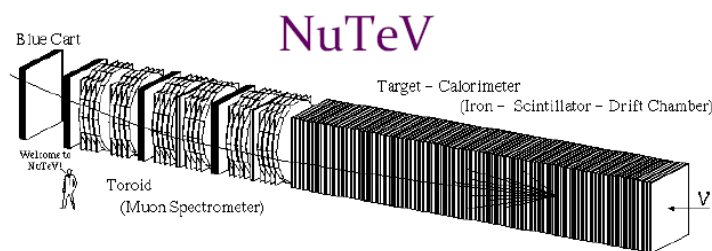


Figure 8: A diagram of the NuTeV detector.

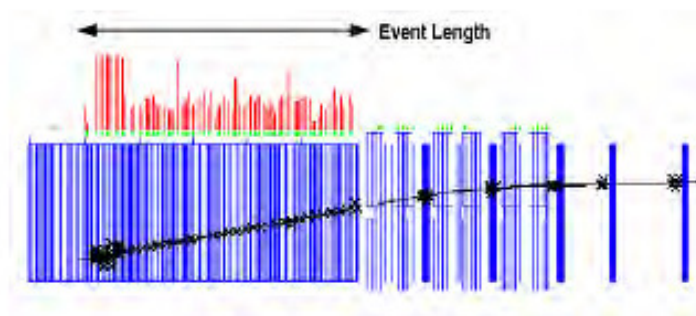


Figure 9: A charged current neutrino interaction in the NuTeV detector, showing the long penetrating muon and the short hadronic splash.

particle identification. As with the tracking detectors, there are many designs and we will not study them.

### 2.4.1 What you need to know

- The main characteristics of this sort of detector.
- How do you do energy measurement?

## 3 Natural Neutrino Sources

In this section we look at the different types of neutrino sources. Neutrinos are produced everywhere : in stars, in supernovae, by the Big Bang. They are generated in gammy ray bursts and in cosmic ray interactions in the atmosphere. The earth generates them in huge numbers as radioactive elements (mostly Uranium and Thorium decay) and we generate them in nuclear reactors and accelerators. Their energies range from micro electron-volts for neutrinos left over from the Big Bang, right up to peta electron-volts for neutrinos produced in violent gamma-ray bursts and Z-bursts in the universe. Figure 10 shows the predicted neutrino flux as a function of neutrino energy from a variety of neutrino sources.

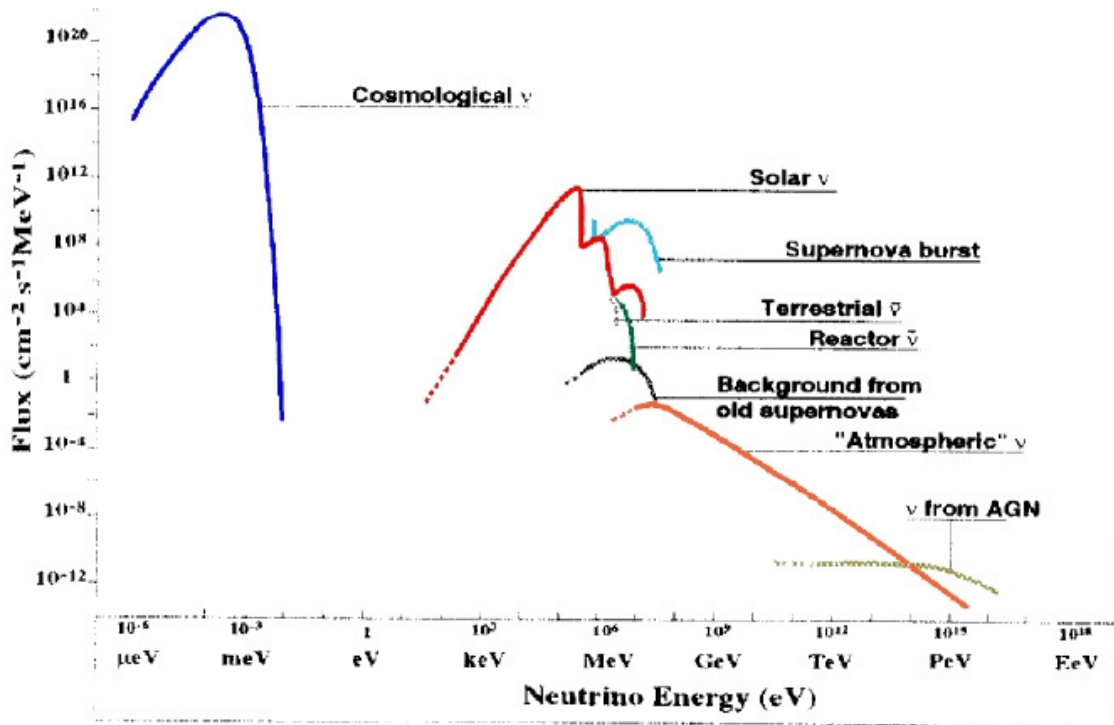


Figure 10: Predicted neutrino flux from most neutrino sources. Note the vast range of energies and fluences.

### 3.1 Relic Neutrinos

This topic has much to do with cosmology and the evolution of the universe. I'm not going to cover this here (that is a lecture course on its own) so will only speak briefly about relic neutrinos.

The evolution of the early universe is a story of cooling as the universe expanded. When the universe was very young and hot, about  $10^{-6}$  seconds after creation all the fundamental particles

composed a thermal soup in which the reactions rates of various particles were in thermal equilibrium. As the universe expands, and the temperature falls, equilibrium can't be maintained and particles *freeze out* or *decouple* from universe evolution. The current picture has electrons, positrons, photons and neutrinos in thermal equilibrium,  $\gamma\gamma \leftrightarrow e^+e^- \leftrightarrow Z^0 \leftrightarrow \nu\bar{\nu}$ , before the universe is a second old. However, after this the temperature falls too far for there to be enough energy to create  $Z^0$  particles and the neutrinos then decouple from the photons and electrons and develop independently. During the next 300,000 years the photons, electrons and positrons are still in thermal equilibrium and the universe is still opaque as photons don't travel far before they scatter off an electron or positron in the plasma. Around 300,000 years after the Big Bang, temperatures have cooled enough to allow electrons to combine with the light nuclei which have been able to form. Once combined, they are no longer in thermal contact with the photons which then evolve independently. At this point the universe becomes transparent. As the universe continues to expand, the temperature decreases and the energy of these photons decreases until today where we know them as the Cosmic Microwave Background. These photons have been studied by the WMAP and COBE satellites and have told us a lot about the structure of the universe at the time when the photons decoupled.

The relic neutrinos, which decoupled after 1 second or so, are also still around. Our model of the universe suggests that they now have energies of around 0.1 meV and are extremely numerous, with about 330 relic neutrinos per cubic centimetre. However, their low energies make them a challenge to detect. They fall below the electron mass, and therefore only interact via the neutral current and, as the neutrino interaction cross section rises linearly with energy direct detection is practically impossible. It is clear, though, that if they were detected they would give us extremely valuable information on conditions of the universe much closer to the Big Bang than our current best probe, the CMB.

### 3.1.1 What you need to know

- That relic neutrinos that are currently undetectable still exist.

## 3.2 Solar Neutrinos

Solar neutrinos are one of the longest standing fields of study in particle astrophysics. Neutrinos are produced copiously by the sun and the only method we have, beside the study of solar oscillations, which give us a direct view into the heart of the solar core.

The sun is a pure generator of electron neutrinos, which arise from the fusion processes which fuel the sun. Although we will not go into the details of stellar energy generation, it is known that the sun generates energy via two fusion chains, known as the PP and the CNO chains.

The p-p chain is responsible for 98.4% of the solar output. In the first reaction of the p-p chain, a proton decays into a neutron in the immediate vicinity of another proton. The two particles form a heavy variety of hydrogen known as deuterium, along with a positron and an electron neutrino. There is a second reaction in the p-p chain producing deuterium and a neutrino by involving two protons and an electron. This reaction (pep-reaction) is 230 times less likely to occur in the solar core than the first reaction between two protons (pp-reaction). The deuterium nucleus produced in the pp- or pep-reaction fuses with another proton to form helium-3 and a gamma ray. About 88% of the time the p-p chain is completed when two helium-3 nuclei react to form an helium-4 nucleus and two protons, which may return to the beginning of the p-p chain. However, 12% of the time, a helium-3 nucleus fuses with a helium-4 nucleus to produce beryllium-7 and a gamma ray. In turn the beryllium-7 nucleus absorbs an electron and transmutes into lithium-7 and an electron neutrino.

Only once for every 5000 completions of the p-p chain, beryllium-7 reacts with a proton to produce boron-8 which immediately decays into two helium-4 nuclei, a positron and an electron neutrino. This is schematically shown in Figure 11.

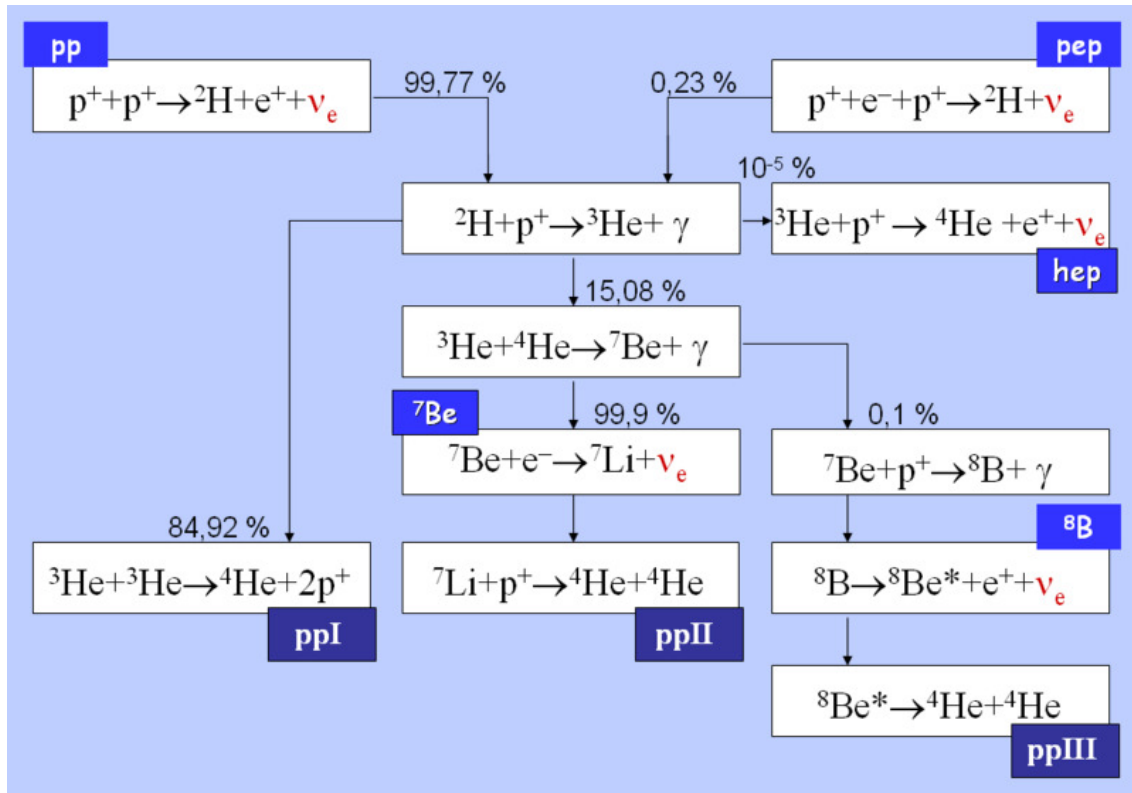
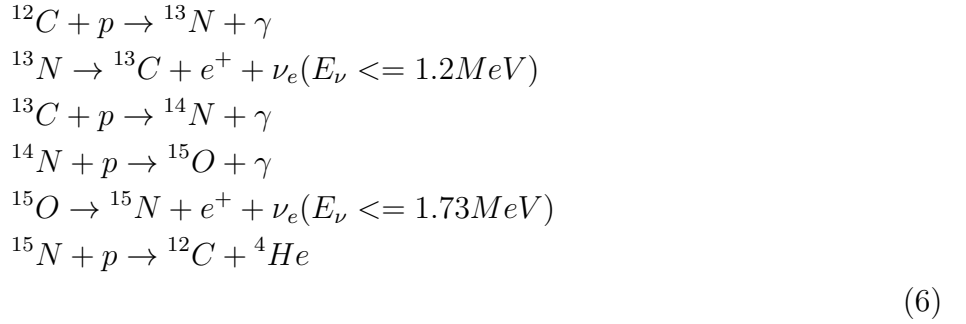


Figure 11: A diagram of the main solar power generation - the PP cycle

The diagram shows each of the different reaction chains that could happen, along with their branching fractions. The electron neutrinos produced in the chain are in red - each of them is given a different name depending on the process which produced them. The primary neutrino produced at the top left is known as the **pp** neutrino, and the one produced at the top right is known as the **pep** neutrino. The neutrino produced in the pp II chain during the beta decay of  ${}^7\text{Be}$  is, not surprisingly, the  ${}^7\text{Be}$  neutrino. At lower right, in the pp III chain, the 15 MeV neutrino produced in the  ${}^8\text{B}$  decay is called the  ${}^8\text{B}$  neutrino. Finally the upper right neutrino is called the **hep** neutrino. Greater than 99.77% of the neutrino flux are pp neutrinos. As we will see most experiments cannot observe these as they are too low in energy.

The other fusion chain is called the Carbon-Nitrogen-Oxygen cycle. As this is only responsible for 1.6% of the solar output we will only mention it briefly. The main reaction steps are:



with the production of two neutrino of energies of 1.2 MeV and 1.73 MeV. This is the last we will mention this cycle.

By modelling the processes that happen in the sun computationally, it is possible to predict the solar neutrino flux as observed on earth. The Standard Solar Model was, in fact, the life work of a man called John Bahcall who died in 2005. The predicted neutrino spectrum from his model is shown in Figure 12. The Standard Solar Model predicts that most of the flux comes from the pp neutrinos with energies below 0.4 MeV. Only the Gallium experiments are sensitive to this component. The Chlorine experiments can just observe part of the  $^7\text{Be}$  line, and can see the other components. The big water experiments (Super-Kamiokande, SNO) can only view the  $^8\text{B}$  neutrinos as they have too high a threshold to see below about 5 MeV.

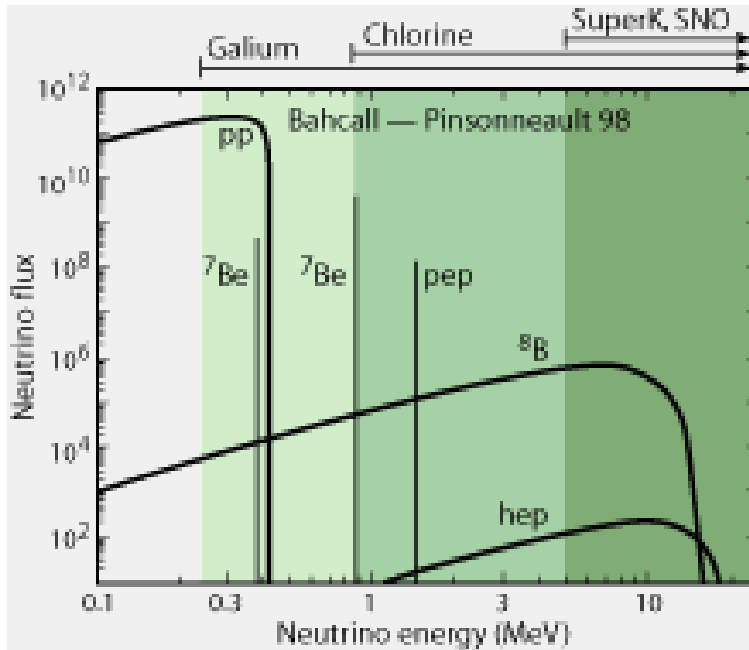


Figure 12: The Standard Solar Model prediction of the solar neutrino flux. Thresholds for each of the solar experiments is shown at the top. SuperK and SNO are only sensitive to Boron-8 and hep neutrinos. The gallium experiments have the lowest threshold and can observe pp neutrinos.

### 3.2.1 The Solar Neutrino Detectors and the Solar Neutrino Problem

We now discuss, briefly, each of the important solar neutrino detectors and their results.

## *Homestake*

Ray Davis' Homestake experiment was the first neutrino experiment designed to look for solar neutrinos. It started in 1965, and after several years of running produced a result for the average capture rate of solar neutrinos of  $2.56 \pm 0.25$  SNU. The big surprise was that the Standard Solar Models of the time predicted that Homestake should have seen about  $8.1 \pm 1.2$  SNU, over three times larger than the measured rate. This discrepancy became known as **the Solar Neutrino Problem**.

At the time it was assumed that something was wrong with the experiment. After all, the Homestake experiment is based on counting very low rate interactions. How did they know that they were seeing solar neutrinos at all? They had no directional or energy information. The objections towards the experiment became harder to maintain when the Super-Kamiokande results were released.

## *Super-Kamiokande*

The main mode of solar neutrino detection in Super-Kamiokande is the elastic scattering channel  $\nu_e + e^- \rightarrow \nu_e + e^-$  which has a threshold of 5 MeV. This threshold comes from the design of the detector - neutrinos with energies less than 5 MeV which elastically scatter in the water will not generate an electron with enough momentum to be seen in the detector. Super-Kamiokande observed a capture rate of about  $0.45 \pm 0.02$  SNU, with a model prediction of  $1.0 \pm 0.2$  SNU, almost a factor of two larger than observation. In addition, since Super-Kamiokande was able to reconstruct the direction of the incoming electron (with some large resolution due to both scattering kinematics - Super-Kamiokande sees the final state electron which isn't quite collinear with the incoming neutrino direction - and to multiple scattering of the final state electron - which smears the directional resolution out even more), it was able to show that the electron neutrinos do indeed come from the sun (see Figure 13).

## *SAGE and GALLEX*

An obvious drawback of both the Chlorine and the water experiments was that they were only sensitive to the relatively rare  $^8B$  and pep neutrinos. The Gallium experiments were able to observe part of the pp neutrino flux. SAGE, which ran with 50 tonnes of Gallium, observed a capture rate of  $70.8 \pm 5.0$  SNU compared to a model prediction of  $129 \pm 9$  SNU. It's counterpart, GALLEX, observed a rate of  $77.5 \pm 8$  SNU. Again the observations were lower than the prediction - this time by about 40%.

A summary of these results is shown in Figure 14.

In all experiments, the model seems to overestimate the solar neutrino capture rate by approximately a factor of two although, crucially, the discrepancy appears to be energy dependent - the lower in energy the experiment is able to probe, the less the discrepancy. Such a discrepancy has two main solutions. One is that our model of the Sun is just wrong, and the other is that there is something wrong with the neutrinos coming from the sun. It turns out to be very difficult to decrease the number of neutrinos being emitted from the sun, in an energy dependent way, by a factor of two, without doing things like switching off the solar output completely, or blowing the sun up. Further, other observations on solar oscillations (essentially sun quakes) agree well with the Standard Solar Model. Attention therefore began to fall upon the neutrinos and recently it was indeed shown that neutrino flavour oscillations were responsible for the experimental results - as we will see later.

### 3.2.2 What you need to know

- How the sun creates energy. Know that there are different types of neutrinos generated in different parts of the pp chain, and also know their energies.



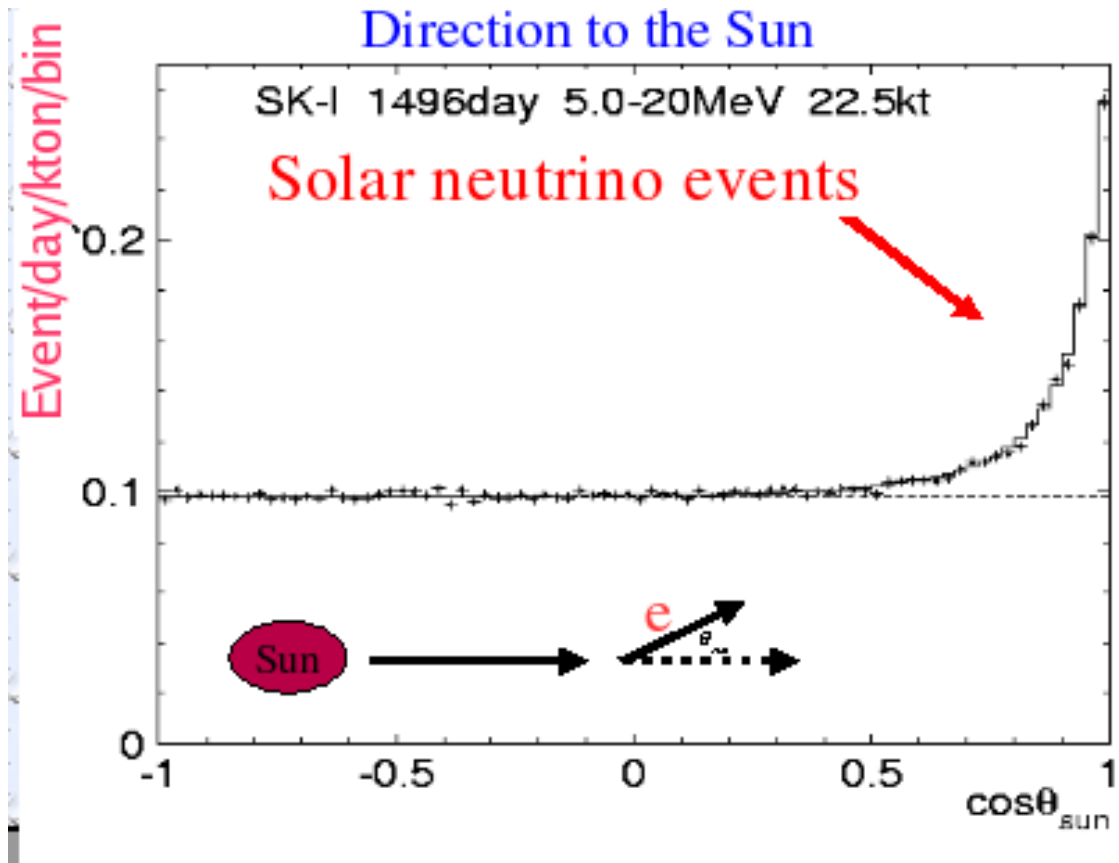


Figure 13: The cosine of the angle between the measured electron in the Super-Kamiokande solar neutrino data, and the direction to the sun at the time the event occurred. A clear peak can be seen for  $\cos\theta > 0.5$  above an essentially flat background. The peak is broad because of kinematic smearing and multiple scattering of the final state electron in the water.

- Which experiments have studied them, their thresholds and what they found.
- What the solar neutrino problem was.

### 3.3 Neutrinos From Supernovae

Amongst the more violent astrophysical events is the Supernova - the explosion of a massive star. During such an event, the star can briefly outshine it's host galaxy, radiating as much energy in a week as the sun radiates in 10 million years. Neutrinos are produced in huge numbers in such a explosion and are extremely valuable. Due to their weak interactions they generally escape the star first, leading to a neutrino shell propagating outwards from the star, which can reach observers (us) often hours before the light does. Hence they are useful probes of the processes occurring in the supernova deep in the core before explosion, and are also alarms that we should direct our telescopes to some region of the sky to be ready when the light arrives. Supernovae can be produced in two ways; either they are caused by thermonuclear explosion of white dwarf stars within a binary system, or by the core collapse of a massive star with mass more than 8 times the solar mass. The mechanism of core collapse is extremely complicated, and we will only describe it briefly here.

**Total Rates: Standard Model vs. Experiment**  
Bahcall-Pinsonneault 2000

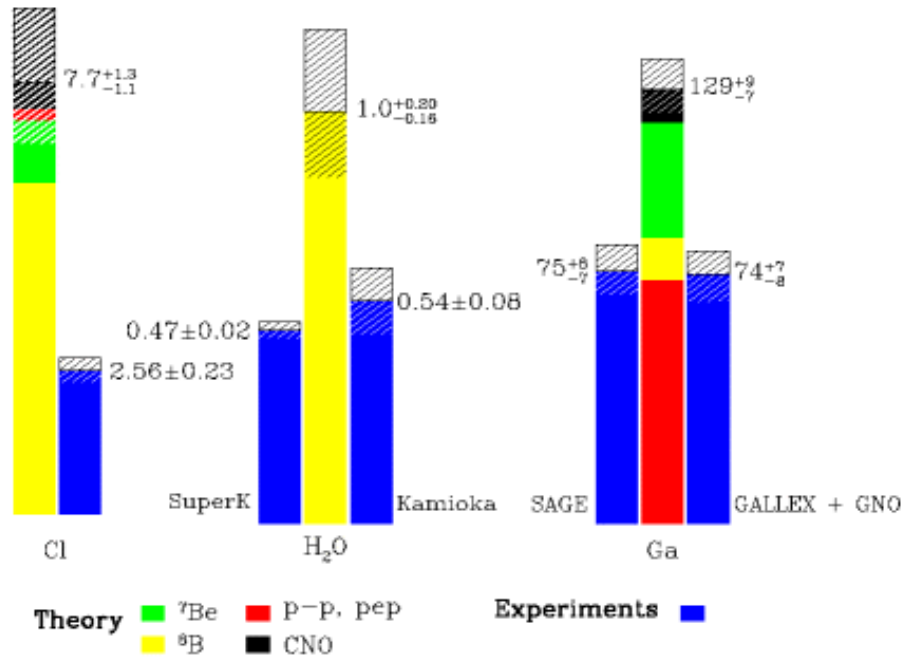


Figure 14: The state of the solar neutrino problem before SNO. Each group of bars represents a different type of experiment : Chlorine on the left, water in the middle and Gallium on the right. The blue bars in each cluster represent the measurements of individual experiments, in SNUs. The middle bar shows the Standard Solar Model prediction. In all cases, the measurements are less than predicted.

### 3.3.1 The evolution of massive stars

A star exists in the hydrogen burning phase described in the previous section on solar neutrinos for tens of millions of years. However, there is only so much hydrogen and eventually the star begins to run out. Hydrogen burning provides the counterbalance to gravitational collapse necessary to keep the star stable. Once the hydrogen runs out, the star begins to contract and the core begins to heat up. If a sufficiently high temperature is achieved, the star begins to burn helium, a byproduct of the old hydrogen fusion process, and swells to become a red giant. After about 10,000 years in this phase the helium in the core also fuses, resulting in carbon, nitrogen and oxygen, and the same cycle begins again - gravitational collapse, core heating and the ignition of a new fusion process with heavier byproducts. The lower temperature fusion processes (H, He) move to the outer regions of the star leading to an onion-like structure, with different fusion processes at different temperatures occurring as one moves radially out from the core. Additional burning phases in the core proceed (see Table 1) until the star is left with just silicon in the core, which it fuses to iron. During the later phases the star radiates most of its energy in neutrinos, rather than photons. This last burning process lasts less than a day, and the star is finally out of options - further energy gain from fusion is impossible. The cycle of pressure increase to temperature increase to fusion reignition to expansion can no longer

Fuel	T (10 <sup>9</sup> K)	Main product	Burning Time	Cooling Process
<sup>1</sup> H	0.02	<sup>4</sup> He, <sup>13</sup> Ni	10,000,000 years	Photons, Neutrinos
<sup>4</sup> He	0.2	<sup>12</sup> C, <sup>16</sup> O, <sup>22</sup> Ne	50,000 years	Photons, Neutrinos
<sup>12</sup> C	0.8	<sup>20</sup> Ne, <sup>23</sup> Na, <sup>28</sup> Mg	600 years	Neutrinos
<sup>20</sup> Ne	1.5	<sup>16</sup> O, <sup>24</sup> Mg, <sup>28</sup> Si	1 year	Neutrinos
<sup>16</sup> O	2.0	<sup>28</sup> Si, <sup>32</sup> S	180 days	Neutrinos
<sup>28</sup> Si	3.5	<sup>54</sup> Fe, <sup>56</sup> Ni, <sup>52</sup> Cr	1 day	Neutrinos

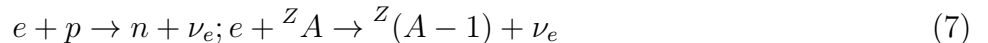
Table 1: The main burning phases of a massive star on its way to a supernova.

proceed.

In the final phase the mostly iron core is kept from collapsing by electron degeneracy pressure. This is a quantum mechanical effect arising from Pauli's exclusion principle, which states that two fermions cannot be in same quantum mechanical state at the same time (e.g. position, energy, spin). From Heisenbergs Uncertainty Principle :  $\Delta x \Delta p >= \frac{\hbar}{2}$ . As matter gets more and more compressed, the uncertainty in the electron position becomes smaller, implying the uncertainty in the electron momentum becomes larger. This uncertainty in the momentum implies that the electrons can exert a pressure on the surrounding matter which can withstand the gravitational collapse.

### 3.3.2 Core Collapse

If the star is massive enough, the electrons in the core can have a high energy (due to the exclusion principle). If this energy is high energy, the electrons can be captured by the protons and heavy nuclei of the core



Unfortunately for the star, this eats the electrons which are staving off collapse and the core begins to contract at supersonic speeds, leaving behind a lot of neutrinos which begin to propagate outwards. Initially these neutrinos can leave the core unhindered, but as densities increase the neutrinos become trapped in the core. The transition between the region in which neutrinos are trapped and the region in which the neutrinos can still propagate is called the *neutrino sphere*. The core continues to collapse until it reaches densities comparable to that of an atomic nucleus. At this point *neutron degeneracy pressure* and strong force interactions halt the collapse, and the infalling matter rebounds producing a shock wave that propagates out of the star (the so-called *core bounce*).

The next phase is still a topic of research. Computer models suggest that this shock wave does not itself cause the explosion. Rather it seems to stall in the outer region of the core. At this point the neutrino shell, still propagating outwards, hits the shock and a small percentage of neutrinos interact in the shock wave, dumping energy and revitalising the shock wave. Essentially it is the neutrino shell which blows the outer layers of the star off the core.

After the explosion, the star is composed of two parts : an inner core where the shock was first formed, consisting of neutrons, protons, electrons and neutrinos, and an outer part which settles in about 0.5-1s, emitting most of its in energy in neutrinos. After 1s, the core - a protoneutron star - is essentially an object by itself. It begins to cool by emitting antineutrinos of all flavours (not just electron) in a 5-10s shell.

Neutrinos carry away about 99% of the released energy of the supernova. At the end one is left with a series of neutrino shells propagating outwards from the, now, neutron star hours ahead of the photon shell. The shells are on the order of 10s thick and the neutrinos have energies in the range of

10 MeV. Detectors on earth in this energy range are most sensitive to the electron-neutrinos which can still undergo charged current interactions. The muon- and tau- neutrinos have too small an energy to produce the respective charged leptons and so can only interact via the neutral current making their detection difficult.

### 3.3.3 Supernova SN1987A

In 1987, a star 150,000 light years away in the Larger Magellanic Cloud was observed to explode. This was the brightest explosion seen since about 1604 and was the first supernova to occur at the same time as neutrino detectors were operating on Earth. In essence this marked the start of a new subfield of particle physics - neutrino astrophysics. Operating at the time were 4 neutrino detectors. Two of them were water Cerenkov detectors (one in South Africa, and one in Japan) and two were liquid scintillator detectors (in France and Russia). In total 24 events were detected (world-wide) within a time window of 12 second, an unprecedented activity rate from 3 far-flung detector. A plot of the time and energy distribution of each event from three of these detectors is shown in Figure 15.

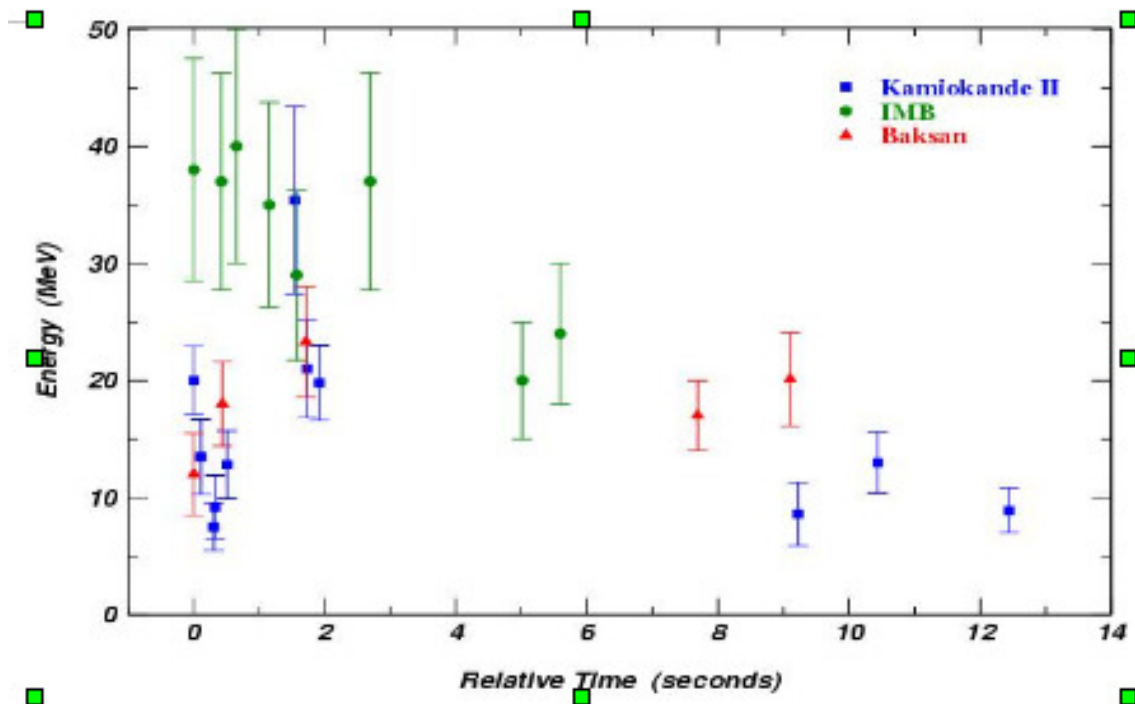


Figure 15: The energies of all neutrino events detected on 23 February 1987, with the time measurement relative to the first event detected.

The following observations were made from the study of this sparse set of 25 events:

- All events were initiated by electron neutrinos.
- The number of observed events implied an electron neutrino flux of  $\Phi = (5 \pm 2.5) \times 10^{-9} \text{cm}^{-2}$ . This is in agreement with the current models. Comparison with the light curves from the other telescopes shows that more than 90% of the energy of the supernova was released in the form of neutrinos.

- The pulse was about 10s wide, as described by the models.
- Since the expected number of neutrinos were measured, none could have decayed on transit, giving a lower limit of the neutrino lifetime of  $1.5 \times 10^5$  years.
- The mass of the electron neutrino must be less than 5.7 eV. This is inferred from the observed spread of the neutrino arrival time distribution, assuming some model dependencies on the initial width of the neutrino shells. If the time of flight ( $t_F$ ) of a neutrino of mass  $m_\nu$  and energy  $E_\nu$  from the source (at time  $t_0$ ) to the detector (arriving at time  $t$ ) is

$$t_F = t - t_0 = \frac{L}{v} = \frac{L}{c} \frac{E_\nu}{\text{sqrt}E_\nu^2 - m_\nu^2 c^4} \approx \frac{L}{c} \left(1 + m_\nu^2 \frac{c^4}{2E_\nu^2}\right) \quad (8)$$

then two neutrinos with energies  $E_1$  and  $E_2$  emitted at time  $t_{01}$  and  $t_{02}$  respectively, will show an arrival time difference on earth of

$$\Delta t = t_2 - t_1 = \Delta t_0 + \frac{Lm_\nu^2}{2c} \left(\frac{1}{E_2^2} - \frac{1}{E_1^2}\right) \quad (9)$$

In the data recovered from SN1987A,  $\Delta t$ ,  $L$ ,  $E_1$  and  $E_2$  are more-or-less known. The mass is unknown, as is the difference between emission times  $\Delta t_0$ . The mass estimate is therefore dependent on assumption in the width of the neutrino pulse at emission.

It's fairly amazing that this much can be inferred from such minimal data. There is now a large collaboration of neutrino experiments all tied into the SuperNova Event Watch System (SNEWS). If any two of the detectors see a large of pulse of neutrinos at the same time, the SNEWS will provide early warning for the astronomers who will then turn their telescopes to observe a given region of the sky. A Supernova going off in our galaxy may well provide signals of more than 5000 electron antineutrinos, with more information both on neutrinos and on supernova processes.

### 3.3.4 What you need to know

- A general understanding of Supernova processes.
- What SN1987A was, and what we found about neutrinos from it.

## 3.4 Other Astrophysical Neutrinos Sources

Neutrinos are not affected by magnetic fields, and interact so weakly that they can free stream from regions where photons would be absorbed. These properties make neutrinos very attractive as a probe of astrophysical phenomena which would otherwise be invisible to earth-based detectors. So attractive, in fact, that the study of neutrinos from astrophysical sources is actually a subfield itself : Neutrino Astrophysics. A full discussion of neutrino astrophysics will not be given here. However, we will briefly discuss several possible sources of high energy neutrinos.

The production of high energy neutrinos splits roughly into two categories : acceleration processes and annihilation in combination with the decay of heavy particles.

### 3.4.1 Neutrinos produced in acceleration processes

Some astrophysical mechanisms are capable of accelerating protons to extremely high energies (sometimes more than  $10^{16}$  GeV. Neutrinos are expected to be associated to these protons via the interaction of the protons with background photons or other protons, generating showers of high energy mesons :  $p + p, p + \gamma \rightarrow \pi^0, \pi^\pm, K^\pm$ . These mesons decay in flight to neutrinos. The neutrinos can be associated either with the interaction of protons with the interstellar medium, and can generate a diffuse constant background, or from the interaction of protons directly in region surrounding the source (so-called “point sources”). Some of the possible point sources which could generate the required acceleration mechanisms are

- **Supernova acceleration** : Acceleration in the expanding supernova shell of a dead star. The acceleration mechanism being the rapidly rotating magnetic field of the remnant neutron star.
- **Black holes and Quasars** : In binary systems, matter can be transferred from a large expanded star to a companion compact object like a black hole. The matter forms an accretion disc around the compact object, which can form powerful acceleration mechanisms under the influence of rotating magnetic fields from the object.
- **Active Galactic Nuclei and Blazars:** Roughly 1% of all bright galaxies contain an active core which radiates energy with a power more than that radiated by the Milky Way. This core is generally concentrated in a region around the size of solar system. This radiation is thought to come from the gravitational release of energy associated with accreting super-massive black holes, and can be directed in jets with powerful shock accelerations (see Figure 16 for a schematic of neutrino generation in such an AGN jet).
- **Gamma Ray Bursts** : The most luminous of violent astrophysical events, these objects outshine supernova by factors of thousands in luminosity, but only last for a short time (milliseconds to minutes). Although not quite understood, GRBs are thought to originate from the core collapse of super-massive stars (so-called “hypernovae”) or from the collision of neutron stars orbiting in a binary system. Whatever the mechanism, GRBs radiate in collimate jets in which ultra-high energy neutrinos could easily be produced.

A different generation mechanism may arise from the decay or annihilation of exotic phenomena left over the Big Bang. Such phenomenon include an array of wierd and wonderful possibilities : cosmic strings, evaporating black holes, magnetic monopoles, quark nuggets, Q-balls *etc.* - most of these are purely theoretical constructs. One of the more pedestrian is the annihilation or decay of supersymmetric particles known as WIMPs (Weakly Interacting Massive Particles), which have been proposed as a generic class of particles that could make up most of the dark matter of the universe. If these WIMPs are massive, they could become trapped in the core of objects like the Sun. If there is a sufficient density of these particles they could then annihilate, producing neutrinos which, when detected, should point right back to their source.

Due to the high energy of the neutrinos and the extremely low flux, a target roughly on the scale of  $1\text{km}^3$  is required. Clearly there is no way to build an independent experiment of this size. However, if the detection technique is water Cerenkov, then parts of the ocean, or the icecaps can be instrumented with photosensors.

## Particle Generation in AGN Jets

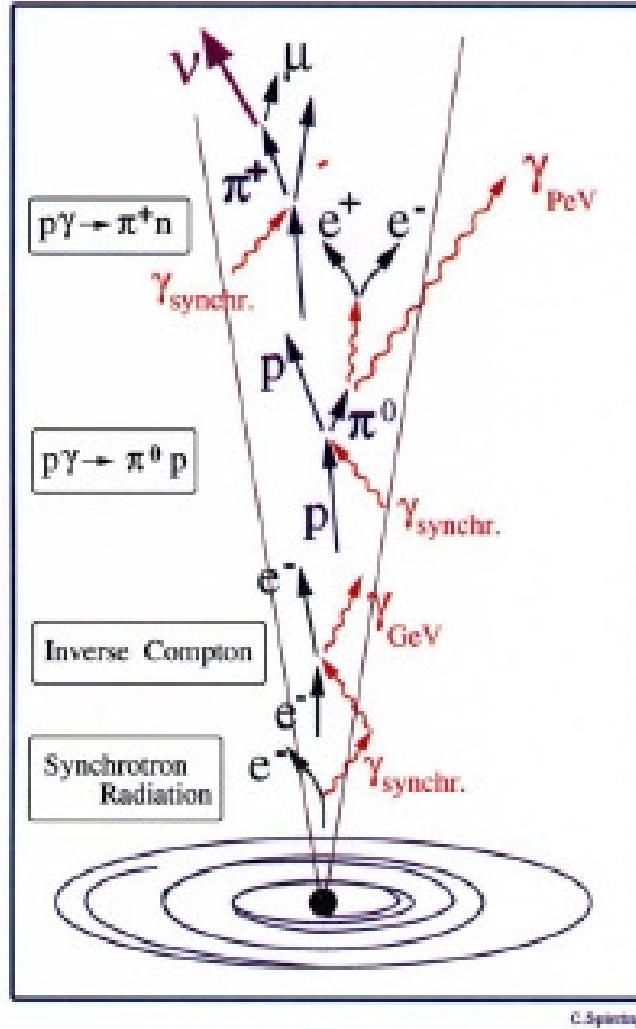


Figure 16: Generation of neutrinos from synchrotron radiation in an AGN jet

### 3.4.2 ANTARES, NESTOR and Baikal

These three experiments are essentially the same in design. A region of sea or a lake with extremely transparent water is selected and strings of photosensors are anchored to the the sea floor. Cerenkov radiation from muons created by the interaction of an astrophysical  $\nu_\mu$  in the earth or atmosphere is detected. The pattern of hits is then used to reconstruct the direction of the muon. At these high energies, the direction of the muon tracks the direction of the neutrino closely, and hence can be used to search for astrophysical point sources.

Baikal is sites in Lake Baikal in Russia at a depth of about 1.1 km, whereas ANTARES and NESTOR are both sites in the Mediterranean at depths of upto 4 km. All are still being constructed.

### 3.4.3 ICECUBE

Water Cerenkov experiments can be performed in ice as well as liquid water. ICECUBE has the goal of instrumenting a cubic kilometre of Antarctic ice with photosensor strings. It is also currently under construction.

### 3.4.4 What you need to know

- Know that neutrinos come from high energy astrophysical sources and the types of detectors we use to detect them
- Why neutrinos are useful in studying these kinds of sources.
- You don't need to know details of the sources.

## 3.5 Geoneutrinos

Geoneutrinos are produced in the decays of unstable, radioactive elements—mostly uranium, thorium, and potassium ( $^{40}K$ )—inside the Earth. These same decays also generate heat, which makes up some portion (thought to be about 60%) of the geothermal heat flow. The amount of geoneutrinos (and radioactive geothermal heat) depends on the amount of radioactive material through the Earth. Although we know the amount and distribution of radioactive material in the Earth's crust well, we have little direct data from the Earth's interior beyond about 10km. Consequently, it remains unclear how much radioactive material is in the bulk of the earth and where it is located. In particular, it is unclear how abundant radioactive elements are in the very core of the Earth. The standard geophysical prediction is that the core is void of all radioactivity. Recently, however, there have been some suggestions that there may be a significant amount of potassium in the Earth's core. These uncertainties about the Earth's radioactive content translate into uncertainties about the amount of geothermal heat and geoneutrinos that are generated by radioactive decays. Thus, measurements of geoneutrinos can address these questions and ultimately determine the nature of the radioactive earth.

Figure 17 shows the energy spectrum of electron antineutrinos produced from several long decay chains in the earth. Notice that the antineutrino energy is very low.

Only recently have experiments been able to probe down to these sorts of energies (at these energies, signals are very small and backgrounds are quite large). In 2005 the KamLAND experiment presented the first ever measurement of geoneutrinos - this represents the first time we have ever been able to probe the interior of the Earth in realtime and opens up a new field of study for geologists. The black line in the plot marks the energy threshold of the KamLAND experiment. It can only observe antineutrinos with energies greater than about 1.8 MeV. That it can see part of the antineutrino flux at all is extremely impressive. The KamLAND data in the low energy part of their spectrum is shown in Figure 18.

The black points represent their data with the thick black line representing their expectation in the absence of geoneutrinos. The coloured lines represent different components of the geoneutrino flux. The dash-dotted blue line is their background (mostly electron antineutrinos generated in nuclear reactors in Japan). The red line represents geoneutrinos from Uranium decay, the green line represent geoneutrinos from Thorium decay, and the brown line represents another background source. The actual number of geoneutrinos KamLAND discovered was on the order of after background subtraction but this was already able to put an upper limit on the heat generation of the earth of about 60



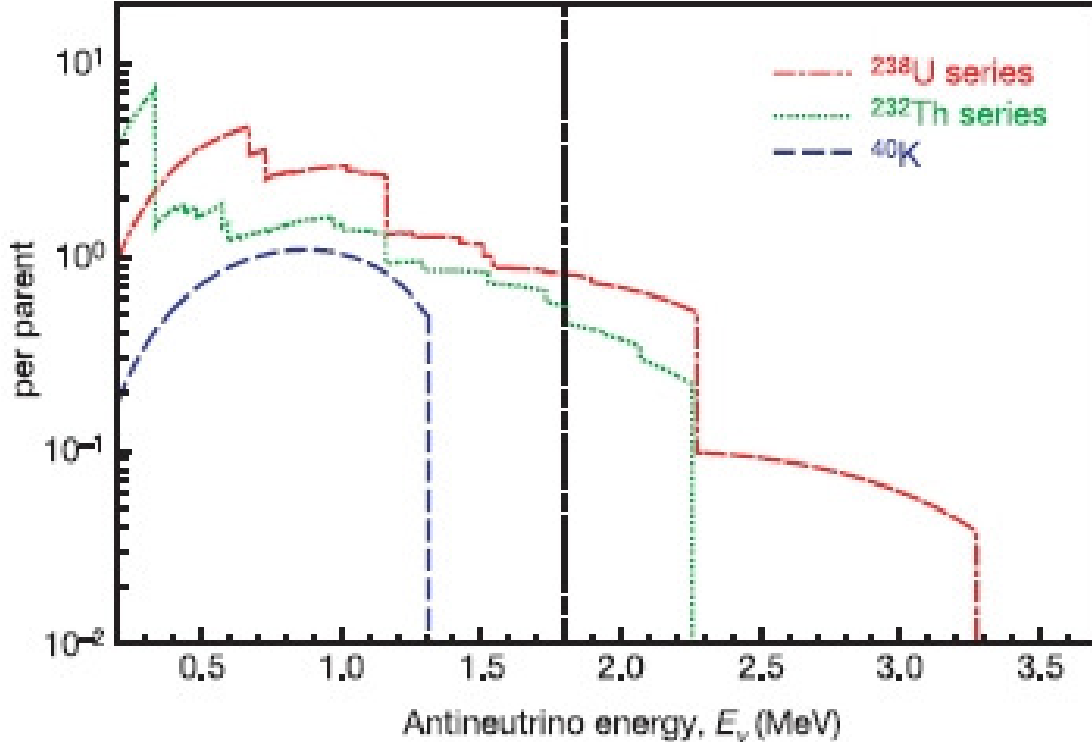


Figure 17: The energy spectrum of electron antineutrinos produced from radioactive decay chains in the Earth’s core. The thick vertical black line shows the energy threshold of the KamLAND experiment which was the first to be able to probe this neutrino source.

Terawatts, thereby providing evidence that there was significant radioactivity in the Earth’s core. This heat drives convection in the Earth’s mantle, and is the driving force behind continental drift and plate tectonics, so a measurement (as imprecise as this is) is extremely valuable.

### 3.5.1 What you need to know

- Know that this source exists, and the broad production mechanism, but no more than that.

## 3.6 Atmospheric Neutrinos

The atmosphere is constantly being bombarded by cosmic rays. These are composed of protons (95%), alpha particles (5%) and heavier nuclei and electrons ( $< 1\%$ ). The energy of the primary particle is shown in Figure 19. For primary energies less than about  $10^{15}$  eV, the spectrum follows a power law of the form  $N(E) \propto E^{-\gamma}$  with  $\gamma \approx 2.7$ . Around  $10^{15}$  eV (called the “knee” region), the spectrum steepens to  $\gamma \approx 3$ . At around  $10^{18}$  eV, the spectrum flattens out again (this is called the “ankle”) region. The region largely responsible for the atmospheric neutrinos is below  $10^{12}$  eV.

When the primary cosmic rays hit nuclei in the atmosphere they *shower*, setting up a cascade of hadrons. The atmospheric neutrinos stem from the decay of these hadrons during flight. The

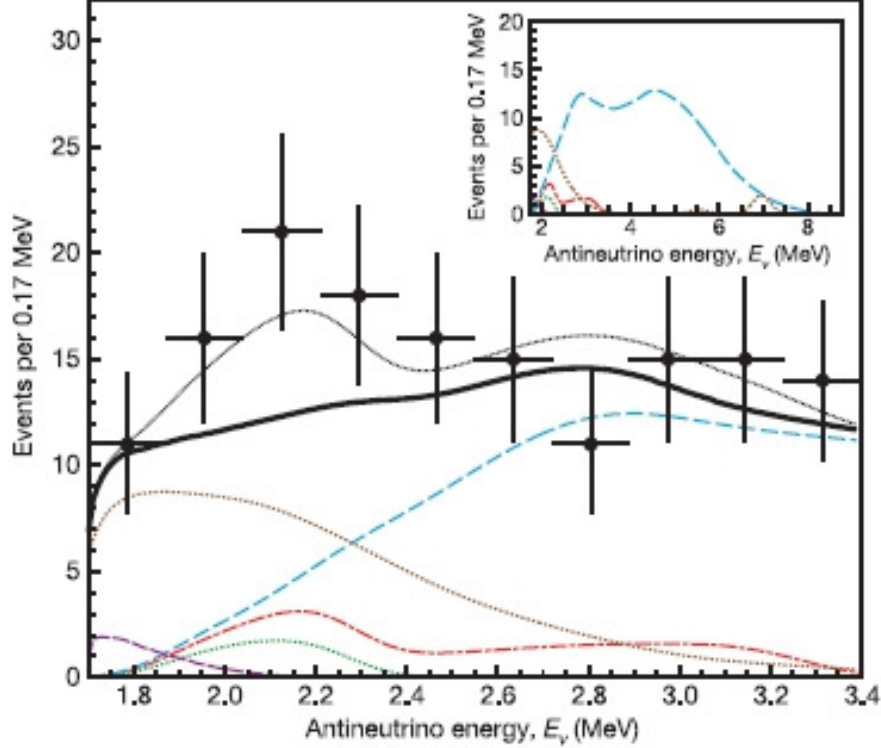


Figure 18: Low energy data collected by KamLAND, showing the small excess of events over background around 2-2.2 MeV indicative of geoneutrinos.

dominant part of the decay chain is

$$\pi^+ \rightarrow \mu^+ \nu_\mu \quad \mu^+ \rightarrow e^+ \nu_e \bar{\nu}_\mu \quad (10)$$

$$\pi^- \rightarrow \mu^- \bar{\nu}_\mu \quad \mu^- \rightarrow e^- \bar{\nu}_e \nu_\mu \quad (11)$$

At higher energies, one also begins to see neutrinos from kaon decay as well. In general the spectrum of these neutrinos peaks at 1 GeV and extends up to about 100s GeV. At moderate energies one can see that the ratio

$$R = \frac{(\nu_\mu + \bar{\nu}_\mu)}{(\nu_e + \bar{\nu}_e)} \quad (12)$$

should be equal to 2. In fact, computer models of the entire cascade process predict this ratio to be equal to 2 with a 5% uncertainty. The total flux of atmospheric neutrinos, however, has an uncertainty of about 20% due to various assumptions in the models.

A detector looking at atmospheric neutrinos is, necessarily, positioned on (or just below) the Earth's surface (see Figure 20). Flight distances for neutrinos detected in these experiments can thus vary from 15 km for neutrinos coming down from an interaction above the detector, to more than 13,000 km for neutrinos coming from interactions in the atmosphere below the detector on the other side of the planet.

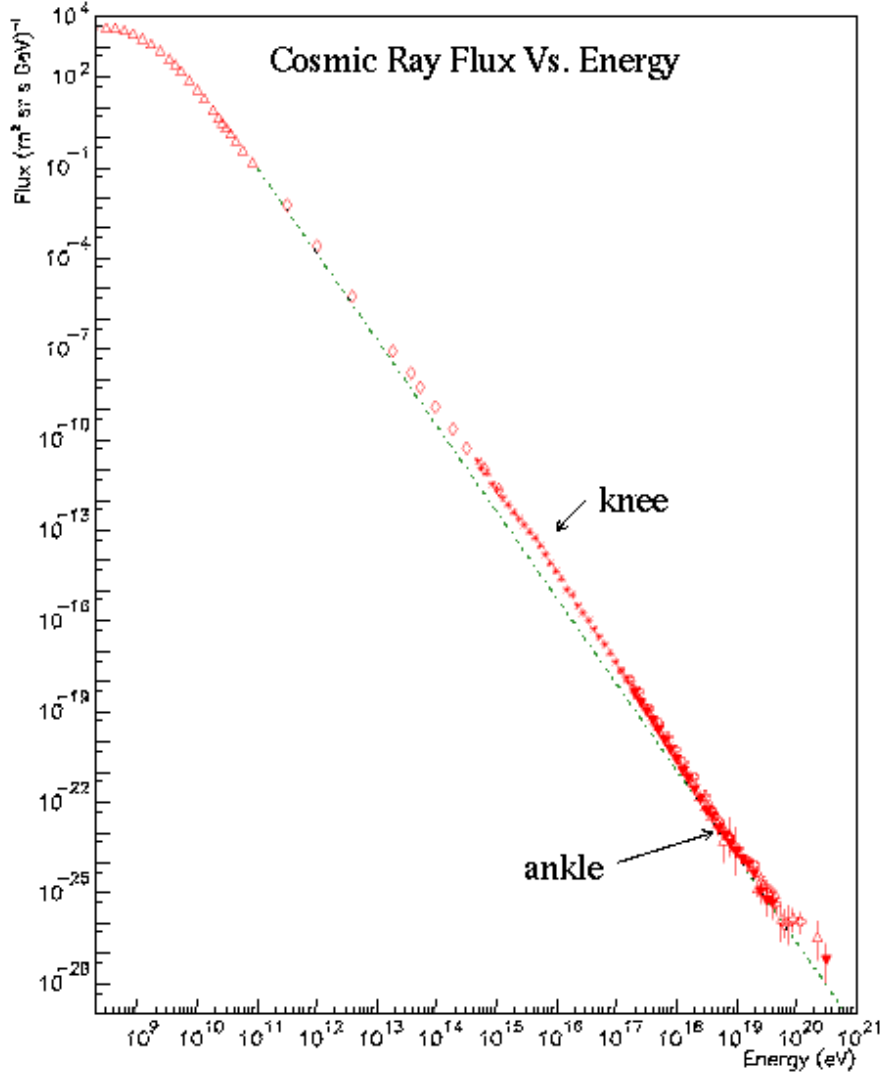


Figure 19: Primary cosmic ray energy spectrum showing the knee and ankle regions.

### 3.6.1 Atmospheric Neutrino Detectors and the Atmospheric Neutrino Anomaly

There have been effectively two categories of detectors used to study atmospheric neutrinos - water Cerenkov detectors and tracking calorimeters. Of the former, the most influential has been Super-Kamiokande (again). We will not discuss the latter.

Atmospheric neutrino experiments measure two quantities : the ratio of  $\nu_\mu$  to  $\nu_e$  observed in the flux, and zenith angle distribution of the neutrinos (that is, the path length distribution). To help interpret the results and to cancel systematic uncertainties most experiments report a *double ratio*

$$R = \frac{(N_\mu/N_e)_{DATA}}{(N_\mu/N_e)_{SIM}} \quad (13)$$

where  $N_\mu$  is the number of  $\nu_\mu$  events which interacted in the detector (called “muon-like”) and  $N_e$  is the number of  $\nu_e$  events which interacted (called “electron-like”). The ratio of  $\frac{N_\mu}{N_e}$  is measured in the data and is also measured in a computational model of the experiment, which incorporates all

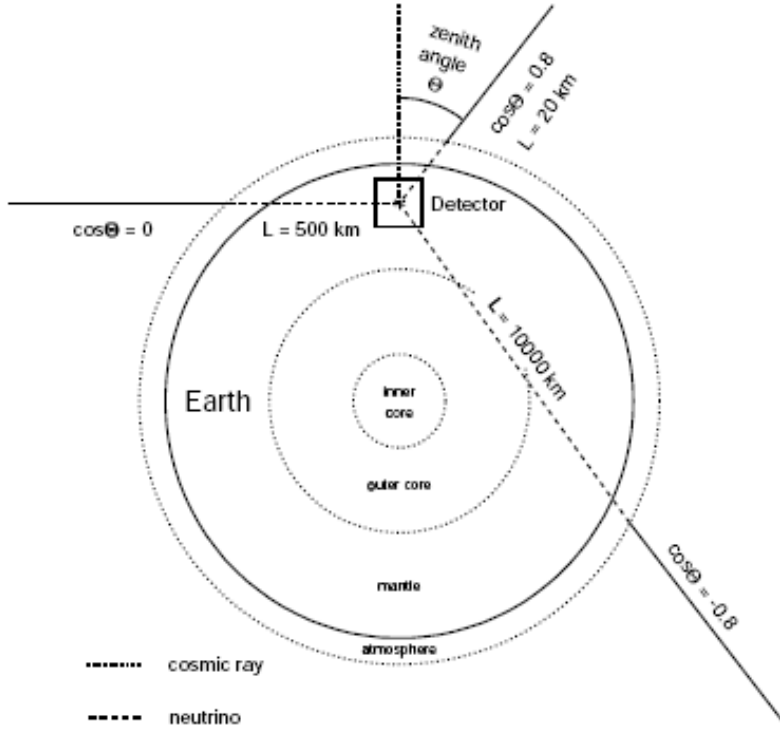


Figure 20: A diagram of an atmospheric neutrino experiment. A detector near the surface sees neutrinos that travel about 15 km looking up, while neutrinos arriving at the detector from below can travel up to 13,000 km. This distance is measured by the “zenith angle”; the polar angle as measured from the vertical direction at the detector :  $\cos\theta_{zen} = 1$  is for neutrinos coming directly down, whereas  $\cos\theta_{zen} = -1$  describes upwards-going neutrinos.

known physics of atmospheric neutrino production, neutrino propagation to the detector and detector response. The absolute flux predictions cancel in this double ratio. If the observed flavour composition agrees with expectation that  $R = 1$ .

A compilation of  $R$  values from a number of different experiments is shown in Table 2. With the exception of Frejus, all measurements of  $R$  are significantly less than 1, indicating that either there was less  $\nu_\mu$  in the data than in the prediction, or there was more  $\nu_e$ , or both. This became known as the **Atmospheric Neutrino Anomaly**.

In addition to low values of  $R$ , Super-Kamiokande was able to measure the direction of the incoming neutrinos. Neutrinos are produced everywhere in the atmosphere and can reach the detector from all directions. In principle, we expect the flux of neutrinos to be isotropic - the same number coming down as going up. The zenith angle distributions from Super-Kamiokande are shown in Figure 21. In this figure, the left column shows the  $\nu_e$  (“e-like”) events, where as the right column depicts  $\nu_\mu$  events. The top and middle rows show low energy events where the neutrino energy was less than 1 GeV, whilst the bottom row shows events where the neutrino energy was greater than 1 GeV. The red line shows what should be expected from standard cosmic ray models and the black points show what Super-Kamiokande actually measured. Clearly, whilst the electron-like data agrees reasonably well with expectation, the muon-like data deviates significantly. At low energies approximately half of the  $\nu_\mu$  are missing over the full range of zenith angles. At high energy the number of  $\nu_\mu$  coming

Experiment	Type of experiment	R
Super-Kamiokande	Water Cerenkov	$0.675 \pm 0.085$
Soudan2	Iron Tracking Calorimeter	$0.69 \pm 0.13$
IMB	Water Cerenkov	$0.54 \pm 0.12$
Kamiokande	Water Cerenkov	$0.60 \pm 0.07$
Frejus	Iron Tracking Calorimeter	$1.0 \pm 0.15$

Table 2: Measurements of the double ratio for various atmospheric neutrino experiments.

down from above the detector seems to agree with expectation, but half of the same  $\nu_\mu$  coming up from below the detector are missing. This was a further indication of flavour oscillations.

### 3.6.2 What you need to know

- How neutrinos are generated in cosmic air showers, and their relative numbers.
- Which experiments study them.
- What was the atmospheric neutrino problem?

We have finished our discussion of natural neutrino sources (finally). The last section discusses artificially produced neutrinos, either from a reactor or from a neutrino beam.

## 4 Artificial Neutrino Sources

### 4.1 Reactors

Nuclear reactors are the strongest source of terrestrial anti-neutrinos, with anti-neutrinos coming from the  $\beta$ -decay arising from unstable fissioning isotopes like  $^{238}\text{U}$  and  $^{239}\text{Pu}$ . Since all the anti-neutrinos come from  $\beta$  decay, reactors can only generate electron-antineutrinos.

The advantage of using reactors as an antineutrino source is that they emit anti-neutrinos isotropically with a flux that falls off as the inverse square distance of the detector from the reactor. This makes the flux prediction far easier than it is in an accelerator environment. In addition, reactors can switch off, allowing detectors to run in beam-on and beam-off mode, greatly facilitating the background estimates.

Electron anti-neutrinos from reactors have energies that peak at around 3 MeV and extend up to about 8 MeV. The energy regime makes scintillator-type detectors ideal for measurement, and any other detector effectively useless. The predominant detection mechanism used by these detectors is the standard inverse beta decay reaction

$$\bar{\nu}_e + p \rightarrow e^+ + n \quad (14)$$

which has a threshold energy of about 1.8 MeV, followed by neutron capture. The main backgrounds come from cosmic rays interactions in the surrounding material, and natural radioactivity. Most scintillator-based detectors of this type have to be *extremely* radiopure.

The classic example of this sort of detector is KamLAND, which used reactors from all over Japan to investigate neutrino oscillations.

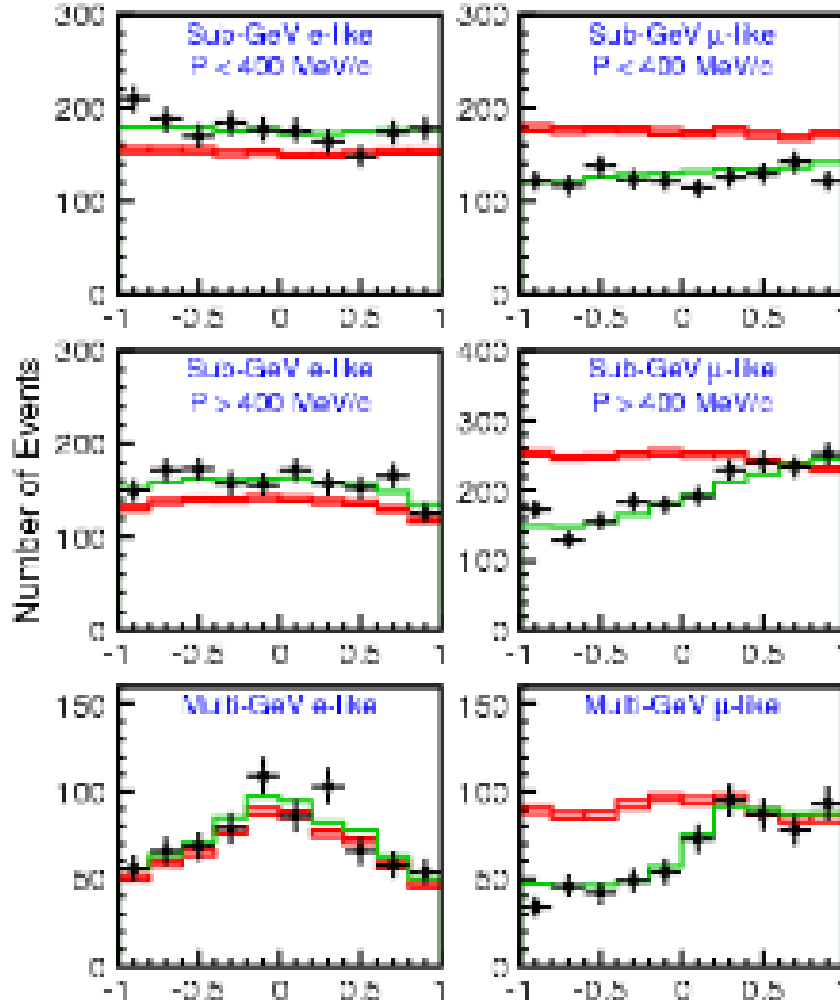


Figure 21: Zenith angle distributions of  $\nu_\mu$  and  $\nu_e$ -initiated atmospheric neutrino events detected by Super-Kamiokande. The left column shows the  $\nu_e$  (“e-like”) events, where as the right column depicts  $\nu_\mu$  events. The top and middle rows show low energy events where the neutrino energy was less than 1 GeV, whilst the bottom row shows events where the neutrino energy was greater than 1 GeV. The red line shows what should be expected from standard cosmic ray models and the black points show what Super-Kamiokande actually measured.

### 4.1.1 What you need to know

- How they are generated in reactors and their energies.

## 4.2 Neutrino Beamlines

To perform many of the measurements that we want to make with neutrinos, we need to be able to produce them artificially and “to order”. It is possible to make neutrinos in accelerators, but it is a complicated process. Conventional neutrino beams are made in much the same way as neutrinos from cosmic ray interactions. A schematic of a beamline is shown in Figure 22

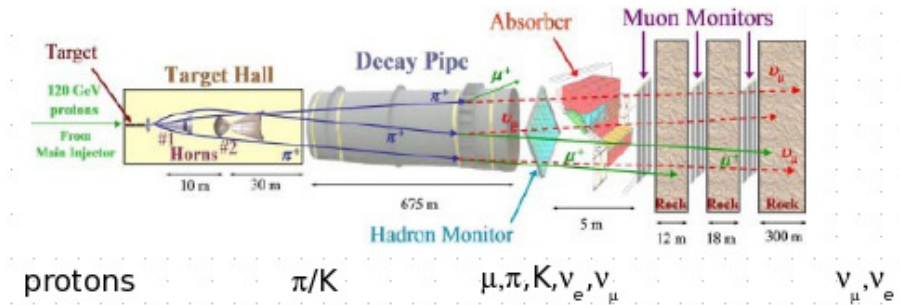


Figure 22: A schematic arrangement of a neutrino beamline.

A proton synchrotron delivers bunches of high energy protons onto a fixed target. The proton collision with the target creates a beam of pions and kaons which enter a magnetic focussing channel which focuses mesons of the correct electric charge into a long, evacuated decay pipe. There the secondaries decay mostly via the reactions (assuming positively charged mesons)

$$M^+ \rightarrow \mu^+ + \nu_\mu (M = \pi, K) \quad (15)$$

Pions decay to muons with a branching ration of 100%. Kaons will decay to muons with a branching fraction of 63.5%. A complication is that the muons can also decay

$$\mu^+ \rightarrow e^+ \bar{\nu}_\mu \nu_e \quad (16)$$

to generate electron neutrinos which one may not want in a pure  $\nu_\mu$  beam.

At the end of the decay tunnel is a long shield designed to absorb mesons which haven’t decayed and stop the charged muons in the beam, letting only the neutrinos through. The experiments are located after the shield.

We look, briefly, at each of the components.

### 4.2.1 Target

The design of a target is a complicated process. Targets have to be strong enough to withstand all the protons that hit them, a process which can cause local heating rates of 1000 degrees in a few microseconds. The target has to be long enough to maximise the probability of the proton to interact. However, the mesons created in the interaction can be re-absorbed or scatter by the target material, so the target has to be short enough to minimise this scattering. These conflicting requirements

also constrain the material the target is made from - heavier to enhance proton interactions, lighter to minimise secondary re-interactions. Figure 23 is a photograph of the target used in the NuMI beamline at Fermilab. The hooks are part of the cooling system and the small black rods are the actual target material, in this case Carbon.



Figure 23: Photograph of the NuMI Target.

Finally, it is crucial that the momentum and angular spectra of the secondary meson be understood, as these have a direct impact on our understanding of the final neutrino spectrum - both in absolute numbers and energy. In fact, imprecise knowledge of these secondary production spectra represents the largest source of error in prediction of the neutrino flux, often up to 30% in absolute rate.

#### 4.2.2 Decay pipe

The decay pipe is basically a big tube. The length of this tube is a function of the energy of the meson that decays in it. The probability that a meson will decay in a pipe of length  $L_D$  is

$$P = 1 - e^{-\frac{L_D}{L_0}} \quad (17)$$

where  $L_0$  is the pion decay length  $\beta\gamma\tau_\pi$ , with  $\beta = \frac{p_\pi}{E_\pi}$ ,  $\gamma = \frac{E_\pi}{m_\pi}$  and  $\tau_\pi$  being the decay time of the pion.  $L_0$  is equal to 55.9 metres  $\times p_\pi/GeV$  for pions and 7.51 metres  $\times p_K/GeV$  for kaons. For a 10 GeV pion, the pion decay length is 559 metres. Hence only about 55% of pions will decay in the decay tube. The more mesons one wishes to decay in the pipe, the longer the decay pipe has to be. Decay pipes can be up to 1 km long for high energy beams.

#### 4.2.3 Energy Spectrum

Neutrino beams can be built to generate neutrinos anywhere between 10 MeV to hundreds of GeV. The scale depends, ultimately, on the energies of the proton beam. The higher the beam energy, the higher the meson energy and the higher the neutrino energy.

The neutrino energy spectrum itself can be determined from the kinematics of the two-body decay of the meson. It can be shown that the energy,  $E_\nu$ , and angle,  $\cos\theta_\nu$ , of the neutrino in the laboratory frame can be related to the same quantities in the meson rest frame by

$$E_\nu = \gamma E_\nu^*(1 + \beta\cos\theta^*) \quad \cos\theta = \frac{\cos\theta^* + \beta}{1 + \beta\cos\theta^*} \quad (18)$$

with

$$\beta = \frac{p_M}{E_M} \quad \gamma = \frac{E_M}{m_M} \quad E_\nu^* = \frac{m_M^2 - m_\mu^2}{2m_M} \quad (19)$$



The minimum and maximum neutrino energies come from cases where the neutrino is emitted backwards and forwards, respectively, in the pion rest frame. That is, when  $\cos\theta^* = \pm 1$ . In this case

$$\begin{aligned}
E_\nu^{min} &= \frac{E_M}{m_M} \frac{m_M^2 - m_\mu^2}{2m_M} \left(1 - \frac{p_M}{E_M}\right) \\
&= \frac{m_M^2 - m_\mu^2}{2m_M^2} (E_M - p_M) \\
&= \frac{m_M^2 - m_\mu^2}{2(E_M^2 - p_M^2)} (E_M - p_M) \\
&= \frac{m_M^2 - m_\mu^2}{2(E_M + p_M)} \\
&\sim \frac{m_M^2 - m_\mu^2}{4E_M} \\
&\sim 0
\end{aligned}$$

and

$$\begin{aligned}
E_\nu^{max} &= \frac{E_M}{m_M} \frac{m_M^2 - m_\mu^2}{2m_M} \left(1 + \frac{p_M}{E_M}\right) \\
&\sim \frac{m_M^2 - m_\mu^2}{m_M^2} E_M \\
&= 0.427 E_\pi \quad \text{for pions} \\
&= 0.954 E_K \quad \text{for kaons}
\end{aligned}$$

where we assume that  $|E| \sim |p|$ . In general, then, neutrino spectra from conventional beams have two components, with the lower energy parts of the beam arising from pion decay, and the higher energy section from kaon decay.

It is fairly easy to show that the neutrino energy at a given angle  $\theta$  in the laboratory is

$$E_\nu(\theta_\nu) \sim E_\nu^{max} \frac{1}{1 + \gamma^2 \theta_\nu^2} \quad (20)$$

For typical experimental configurations, in which  $\theta_\nu$  is small, the experiment sees only the high energy part of the beam. Lower energy beams can usually only be derived by going to lower proton energies so that the meson energies are lower. The limiting type of experiment is to look at pions which do decay at rest - resulting in neutrino beams with energies of tens of MeV. Another, more interesting option, is to go off-axis and view the beam at a different angle  $\theta$ . We will look at this briefly in a minute.

Two types of conventional beams can be produced - wide-band beams (WBB) and narrow-band beams (NBB) which are distinguished by the type of magnetic focussing they use.

#### 4.2.4 Wide Band Beams

Wide band beams use a system of “magnetic horns” to focus the mesons into the decay pipe. These are metal conductors which are pulsed with large (about a few hundred kiloamps) currents synchronously with the beam.

Consider a diverging beam which one wants to focus (see Figure 24). When the particles in the beam hit the lens, they have a transverse momentum proportional to its radius from the centre of the lens. We therefore need a focussing system which bends the particles on the outside of the divergence cone more and those on the inside less. The solution is the device shown in Figure 25. Current flows down the outer sheet of conductor, and returns along the inner sheet - generating a toroidal magnetic field between the sheets. Particles which have a high transverse momentum on the edge of the beam spend a longer time in the field. They are focussed more than the particles in the center of the horn which spend no time in the magnetic field at all. Judicious choice of the shape of the inner conductor (and lot's of modelling) will generate a parallel beam coming out of the horn.

In many cases, one horn is not enough, and mesons can be over-focussed. In order to deal with this a second horn, generally called a “reflector”, is often installed behind the horn to re-correct the beam.

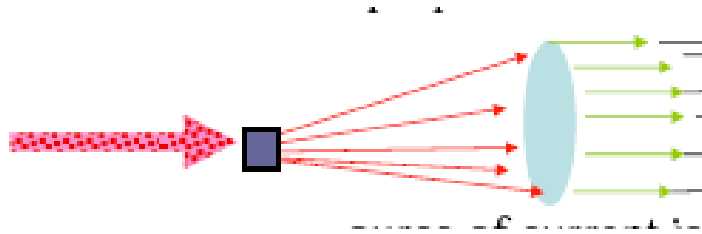


Figure 24: Focusing a diverging beam.



Figure 25: Idealised schematics of a magnetic horn. The dotted line shows the surface of the inner conductor.

The advantage of wide band beams is that one gets a large flux of neutrinos, as almost all mesons produced from the proton interaction are channelled into the decay pipe. The disadvantage is that the final neutrino energy spectrum is a convolution of the decays from different radii and longitudinal points in the decay pipe. The spectra from different mesons are mixed as well so the final spectrum one sees is a sum of the spectra from all mesons. The only way to predict the neutrino spectrum is usually to do a full simulation of the beam process, from proton collision down to detector.

#### 4.2.5 Narrow Band Beams

A schematic of a narrow band beam is shown in Figure 26. It contains all the components discussed above, but using a sophisticated magnetic channel it selects and focuses particles of a particular charge

with a small momentum range, usually with a momentum bite of about  $\frac{\Delta p_M}{p_M} \sim 5\%$ , into the decay pipe. In other words, only mesons of a given momentum are allowed into the decay pipe. Since higher energy mesons decay in the more downstream parts of the pipe, there is a relationship between the energy of the neutrino and the radial distance from the beam axis of a neutrino interaction in the detector.

Since there are both pions and kaons in the beam, which will be focussed into the decay pipe with different energies, narrow band beams tend to be *dichromatic* - with two regions coming from the pions and kaons. An example beam spectrum taken from a real NBB beam at CERN is shown in Figure 27. The plot shows the neutrino energy observed in a detector as a function of the radial distance from the beam axis. Two regions can be seen, the lower one coming from pions, and the upper one coming from kaons. The regions are smeared somewhat as the mesons do not decay at a single point but in a line down the decay pipe.

The advantage of narrow band beams is that one obtains a reasonable flat neutrino spectrum with minimal structure. One can estimate the neutrino energy from the radial position in the beam and there is a small contamination from other mesons. The disadvantage is that the magnetic channel obviously removes most of the mesons that will produce neutrinos, so the flux is orders of magnitude smaller than those in wide-band beams.

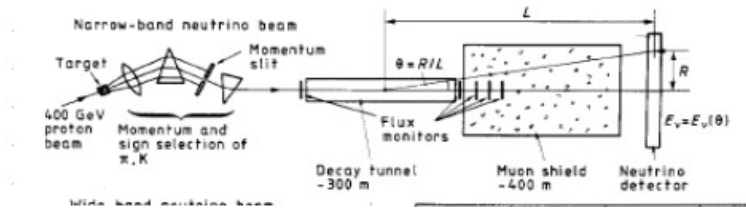


Figure 26: Schematic of a narrow band beam.

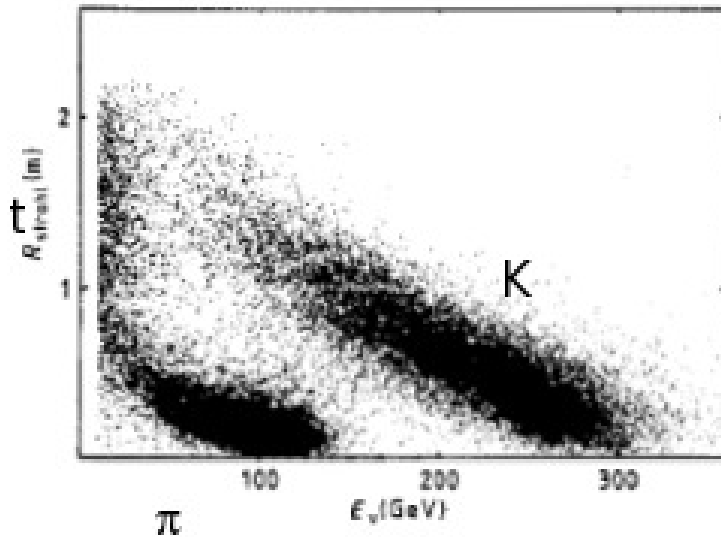


Figure 27: Neutrino energy spectrum from the CDHS narrow band beam at CERN.

### 4.3 Off-axis beams

The new generation of neutrino beams that are currently either being constructed or in the planning stage are built on the foundation of extremely intense proton beams. Studies of neutrino oscillations ideally require a monochromatic neutrino spectrum (i.e. neutrinos of a single energy) and so the drive is towards creating beams which will be monochromatic.

One of the ways to do this is to go off-axis. That is, to position the experiment, not on the beam axis, but at an angle to it. We saw above that the neutrino energy from meson decay as a function of angle is

$$E_\nu(\theta_\nu) \sim \frac{0.43E_\pi}{1 + \gamma^2\theta_\nu^2} \quad (21)$$

where  $\gamma = \frac{E_\pi}{m_\pi}$ . On the beam-axis,  $E_\nu(0) \propto E_\pi$ . As one moves away from the axis, the neutrino energy spectrum turns over and becomes almost flat as shown in Figure 28. Referring to the figure, if one puts a detector at 2 degrees off-axis, the neutrino spectrum becomes almost monochromatic with an energy of 700 MeV.

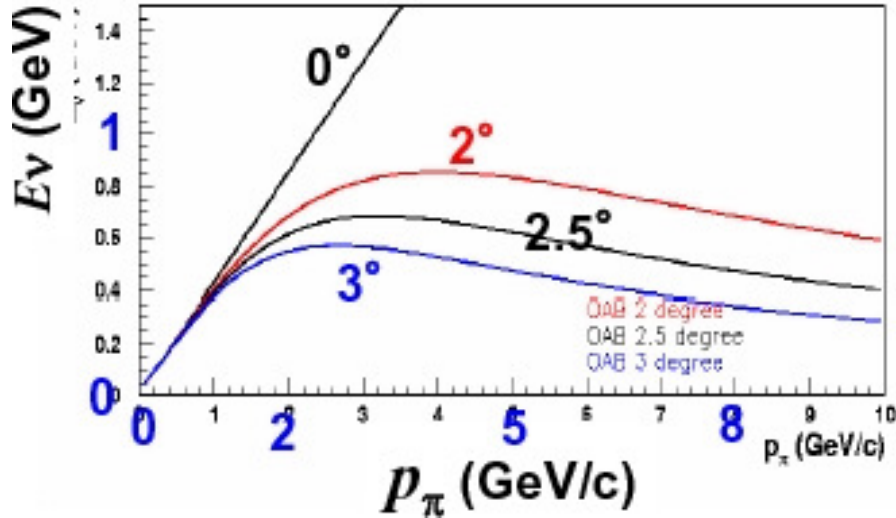


Figure 28: Neutrino energy spectrum as a function of the parent pion momentum at different angles.

Can we show this? Consider the meson decay shown in Figure 29. 4-momentum conservation implies that

$$p_\pi = p_\mu + p_\nu$$

or

$$p_\mu = p_\pi - p_\nu$$

Squaring yields

$$p_\mu^2 = (p_\pi - p_\nu)^2 = p_\pi^2 + p_\nu^2 - 2p_\pi p_\nu$$

Since  $p_\mu^2 = m_\mu^2$ ,  $p_\pi^2 = m_\pi^2$  and  $p_\nu^2 = 0$ , we have

$$\begin{aligned} m_\mu^2 &= m_\pi^2 - 2(E_\pi E_\nu - \mathbf{p}_\pi \cdot \mathbf{p}_\nu) \\ &= m_\pi^2 - 2E_\nu(E_\pi - |\mathbf{p}_\pi| \cos\theta) \end{aligned}$$

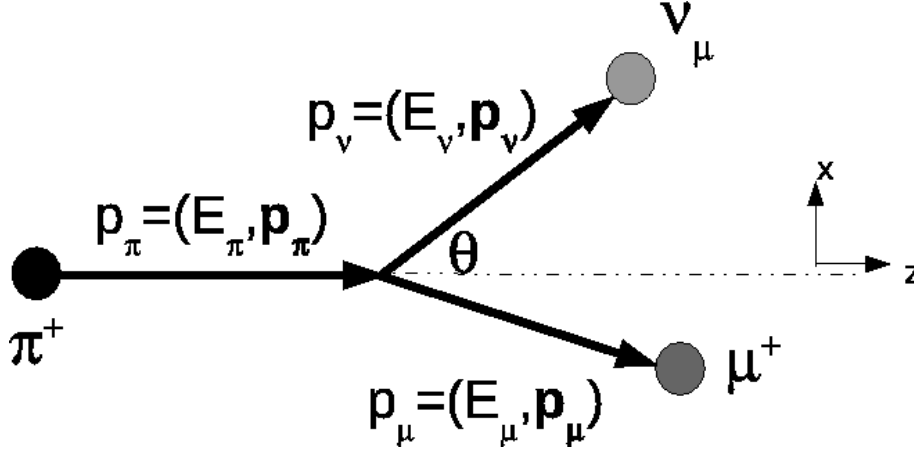


Figure 29: Two-body decay of a meson in a neutrino beamline.

where in the last step we have used  $|\mathbf{p}_\nu| = E_\nu$ . Rearranging gives

$$E_\nu = \frac{m_\pi^2 - m_\mu^2}{2(E_\pi - |\mathbf{p}_\pi| \cos\theta)}$$

Now, the pion momentum is

$$|\mathbf{p}_\pi| = \sqrt{E_\pi^2 - m_\pi^2} = E_\pi \sqrt{1 - \frac{m_\pi^2}{E_\pi^2}} \approx E_\pi \left(1 - \frac{m_\pi^2}{2E_\pi^2}\right)$$

in the limit that  $E_\pi \gg m_\pi$  For small angles,  $\cos\theta \sim 1 - \frac{\theta^2}{2}$ , so the neutrino energy can be written as

$$\begin{aligned} E_\nu &= \frac{m_\pi^2 - m_\mu^2}{2(E_\pi - |\mathbf{p}_\pi| \cos\theta)} \\ &= \frac{m_\pi^2 - m_\mu^2}{2(E_\pi - E_\pi(1 - \frac{m_\pi^2}{2E_\pi^2})(1 - \frac{\theta^2}{2}))} \end{aligned}$$

Replacing  $\frac{E_\pi}{m_\pi}$  by  $\gamma$ , and expanding the product in the denominator we get

$$\begin{aligned} E_\nu &= \frac{m_\pi^2 - m_\mu^2}{2E_\pi(1 - (1 - \frac{1}{2\gamma^2})(1 - \frac{\theta^2}{2}))} \\ &= \frac{m_\pi^2 - m_\mu^2}{2m_\pi} \frac{m_\pi}{E_\pi(1 - (1 - \frac{1}{2\gamma^2} - \frac{\theta^2}{2} + \frac{1}{2\gamma^2} \frac{\theta^2}{2}))} \\ &= \frac{m_\pi^2 - m_\mu^2}{2m_\pi} \frac{1}{\gamma} \frac{1}{\frac{1}{2\gamma^2} + \frac{\theta^2}{2}} \end{aligned}$$

where, in the last step, we only keep first order terms. Multiplying the numerator and denominator by  $1 = \frac{2\gamma^2}{2\gamma^2}$ , We are left with

$$E_\nu = \frac{m_\pi^2 - m_\mu^2}{m_\pi} \frac{\gamma}{1 + \gamma^2 \theta^2}$$

Now,  $\gamma$  is proportional to  $E_\pi$ , so to show that  $E_\nu$  is independent of  $E_\pi$  we need to differentiate the relationship with respect to  $\gamma$  :

$$\frac{\partial E_\nu}{\partial \gamma} = \frac{m_\pi^2 - m_\mu^2}{m_\pi} \frac{1 - \gamma^2 \theta^2}{(1 + \gamma^2 \theta^2)^2}$$

At an off-axis angle of  $\theta = \frac{1}{\gamma}$ , this is

$$\frac{\partial E_\nu}{\partial \gamma} = 0$$

Hence, at  $\theta = \frac{1}{\gamma}$ , the neutrino energy spectrum is independent of the parent pion energy. This angle (in the lab frame) corresponds to a decay angle of 90 degrees in the centre of mass frame. So, given an average pion momentum, if one puts the detector at an angle of  $\frac{1}{\gamma}$  to the beam direction, the energy spectrum of neutrinos will be approximately monochromatic with a central value of

$$E_\nu \sim \gamma \left( \frac{m_\pi^2 - m_\mu^2}{m_\pi} \right)$$

Alternatively, if you know the average pion momentum, you can tune the central energy of the beam by looking at different angles  $\theta$ .

#### 4.3.1 What you need to know

- How neutrinos are generated at accelerators.
- Details of the individual parts of the neutrino beam - what are they used for?
- The differences between wide-band, narrow-band and off-axis beams

## 5 What you should know (Summary)

This is a big section and I surely do not expect you to know everything. As a rough guide though

- Know the mechanism for the different types of detection techniques and what distinguishes them. For example, you should be able to answer the question : *what information will water Cerenkov experiments give you that radiochemical experiments cannot?*
- Understand what mechanism these experiments use : the Homestake experiment, Super-Kamiokande, SNO, KamLAND, and IceCube.
- Be clear on what distinguishes Super-Kamiokande from SNO.
- Understand the following neutrino production mechanisms : solar neutrinos, atmospheric neutrinos, reactors and accelerator production. Detailed understanding is not required, of course, but know the general properties of each mechanism.
- Be familiar with the Solar and Atmospheric Neutrino Problems.
- Be able to give general descriptions of wide-band, narrow-band and off-axis beams.